epithelium of the BMT recipients (Figure 6C). Serial section analysis using CD45, CD10,[35] and cytokeratin immunostaining with Y-FISH revealed the presence of BM-derived absorptive cells expressing CD10 within the intestinal epithelium of the BMT recipients (Figure 6D). These findings suggested that BM-derived cells distribute as all 4 lineages of terminally differentiated epithelial cells associated with lineage-specific functions. However, the dividing potential of the BM-derived epithelial cells is extremely limited, suggesting that new BM cells are constantly being recruited, which in turn mature into terminally differentiated cells after a short residence within the epithelium.

BM-Derived Epithelial Cells Distributed as Secretory Lineage Epithelial Cells Within the Regenerative Epithelium Following GVHD

We have previously shown that BM-derived epithelial cells increase in number and contribute to tissue regeneration in the recovery phase from GVHD.[9] However, whether this increase is correlated with a change in the proliferation and/or differentiation of the BM-derived epithelial cells remains unclear. If the substantial increase of BM-derived cells is due to the increased proliferation of BM-derived epithelial cells within the epithelium, the frequency of Ki-67–positive BM-derived cells should also be increased in BMT recipients who developed GVHD. Thus, we first compared the expression of Ki-67 within BM-derived epithelial cells in BMT recipients who did (GVHD [+]) or did not develop GVHD (GVHD [−]). We also compared the expression in GVHD (+) BMT recipients with or without regenerative epithelium. The total number of BM-derived epithelial cells was substantially increased in GVHD (+) recipients, as compared with GVHD (−) recipients: GVHD (−), 0.76%; GVHD (+) regenerative epithelium (−), 0.97%; GVHD (+)/regenerative epithelium (+), 1.31% of total epithelial cells. The low frequency observed in GVHD (−) recipients was compatible with previous reports.[36] Analysis of the expression of Ki-67 showed that the proportion of Ki-67–positive BM-derived epithelial cells among all Ki-67–positive epithelial cells increased substantially in GVHD (+) recipients with regenerative epithelium, as compared with GVHD (−) recipients or GVHD (+) recipients without regeneration, along with the total number of BM-derived epithelial cells. However, the increase observed in GVHD (+) recipients with regenerative epithelium was not statistically significant compared with GVHD (−) recipients: GVHD (−), 1.0 ± 0.23 cells; GVHD (+)/regenerative epithelium (−), 1.2 ± 1.7 cells/100 Ki-67-positive cells, $P > .1$; GVHD (+)/regenerative epithelium (+), 1.9 ± 1.17 cells/100 Ki-67–positive cells, $P = .076$. These results suggest that BM-derived epithelial cells increase in number via increase of Ki-67–expressing epithelial cells in case of severe intestinal inflammation and the following regeneration of the damaged epithelium but rapidly become resident as terminally differentiated intestinal cells. We next examined whether the increase of BM-derived epithelial cells during regeneration from GVHD is correlated with a change in lineage distribution of the BM-derived epithelial cells. For this purpose, we compared the expression of lineage markers

Figure 6. BM-derived epithelial cells express markers of functional, terminally differentiated epithelial cells within the human intestine. (*A*) A single section of a small intestinal specimen taken from a female BMT recipient was subjected to double-staining analysis to detect BM-derived goblet cells. The section was first stained by Y-FISH and subsequently with alcian blue. Expression of cytokeratin and the absence of CD45 were confirmed by the immunostaining. Of a total of 30,973 epithelial cells examined, 4151 cells were positive for alcian blue, and 26 cells (*arrow*) were double positive (*right 4 panels*; original magnification 19,200×). *Right 4 panels* represent the magnified view of the area indicated by the *yellow square* in the *left end panel* showing the lower magnification view of cytokeratin staining (original magnification, 3200×). (*B*) A single section of a small intestinal specimen taken from a female BMT recipient was subjected to double-staining analysis to detect BM-derived Paneth cells. The section was first stained with H&E to demonstrate the specific eosinophilic granules and subsequently stained by Y-FISH. Expression of cytokeratin and the absence of CD45 were confirmed by the immunostaining. Of a total of 30,973 epithelial cells examined, 428 cells were positive for Paneth cell–specific granules, and a single cell (*yellow arrow*) was double positive (*right 4 panels*; original magnification, 19,200×). *Right 4 panels* represent the magnified view of the area indicated by the *yellow squares* in the *left 2 panels* showing the lower magnification view of H&E or cytokeratin staining (original magnification, 3200×). (*C*) Serial section analysis of small intestinal sections taken from a female BMT recipient was performed to detect BM-derived neuroendocrine cells. Sections were examined by immunostaining for chromogranin A, cytokeratin, CD45, and Y-FISH (*arrow*). Of a total of 30,973 epithelial cells, 1074 cells were chromogranin A positive, and 14 cells were double positive for chromogranin A and Y-FISH (*right 4 panels*; original magnification, 12,800×). *Right 4 panels* represent the magnified view of the area indicated by the *yellow square* in the *left end panel* showing the lower magnification view of cytokeratin staining (original magnification, 3200×). (*D*) Serial section analysis of small intestinal sections taken from a female BMT recipient was performed to detect BM-derived absorptive cells. Sections were examined by immunostaining for CD10, cytokeratin, CD45, and Y-FISH (*arrow*). Of a total of 30,973 epithelial cells, 15,968 cells were CD10 positive, and 159 cells were double positive for CD10 and Y-FISH (*right 4 panels*; original magnification, 12,800×). *Right 4 panels* represent the magnified view of the area indicated by the *yellow square* in the *left end panel* showing the lower magnification view of cytokeratin staining (original magnification, 4800×).

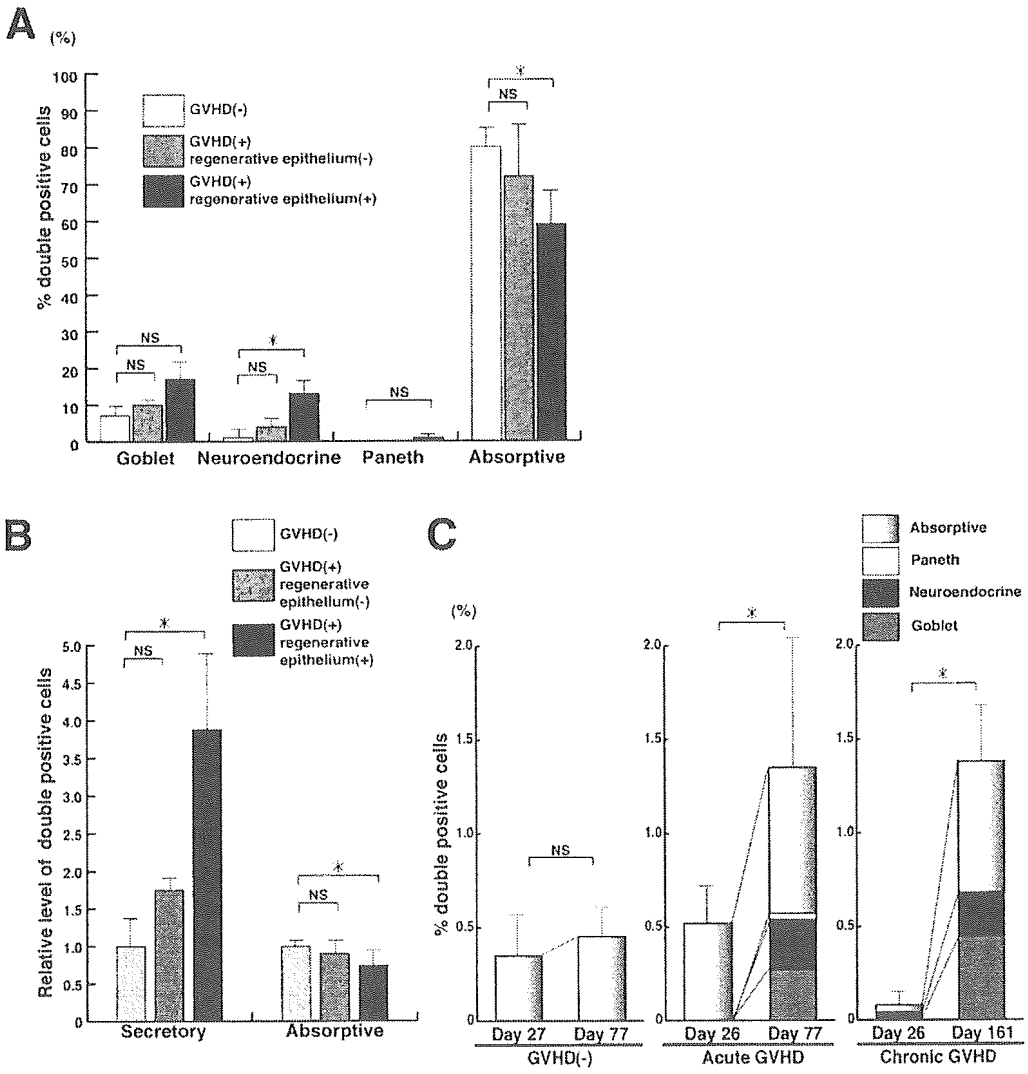

Figure 7. BM-derived epithelial cells proliferate and increase as secretory lineage cells in the regenerative epithelium following GVHD. (*A*) Coexpression of lineage-specific differentiation markers within BM-derived epithelial cells was compared in the same 3 groups of patients: patients who did not develop GVHD (*GVHD* (−), 13,629 epithelial cells); patients who developed GVHD but without regenerative epithelium (*GVHD* (+)/*regenerative epithelium* (−), 2976 epithelial cells); and patients who developed GVHD accompanied with regenerative epithelium (*GVHD* (+)/*regenerative epithelium* (+), 7114 epithelial cells). Coexpression of the lineage-specific markers was examined in a total of 239 Y-FISH–positive epithelial cells by analysis of serial sections or double staining of a single section, as formerly described. BM-derived neuroendocrine cells showed a significant increase, whereas BM-derived goblet cells and BM-derived Paneth cells also showed substantial increase in GVHD (+)/regenerative epithelium (+) compared with GVHD (−). In sharp contrast, BM-derived absorptive cells showed a significant decrease in GVHD (+)/regenerative epithelium (+) compared with GVHD (−). GVHD (+)/regenerative epithelium (−) showed no significant difference compared with GVHD (−). Values are shown as mean ± SE. *Indicates $P < .05$. NS indicates $P \geq .05$. (*B*) Coexpression of secretory cell lineage or absorptive lineage markers within BM-derived epithelial cells was compared in the same 3 groups of patients. The results in Figure 7*B* were reanalyzed in terms of secretory or absorptive lineage, and data were presented as the relative level of each lineage within BM-derived cells compared with GVHD (−). Secretory lineage cells were found to be significantly increased, whereas absorptive lineage cells were significantly decreased in GVHD (+)/regenerative epithelium (+). GVHD (+)/regenerative epithelium (−) showed no significant difference compared with GVHD (−). Values are shown as mean ± SE. *Indicates $P < .05$. NS indicates $P \geq .05$. (C) Series of biopsy specimens taken at different time points post-BMT from 3 cases were examined for coexpression of lineage-specific differentiation markers in BM-derived epithelial cells. A case that did not develop GVHD (*GVHD* [−]) showed no increase of BM-derived epithelial cells between day 27 (3235 total epithelial cells) and day 77 (1790 total epithelial cells), and the differentiated BM-derived epithelial cells were dominated by absorptive lineage cells. In sharp contrast, a case that developed acute GVHD around day 77 post-BMT showed a significant increase in the frequency of BM-derived epithelial cells between day 26 (968 total epithelial cells) and day 77 (3870 total epithelial cells). This increase was associated with a substantial increase of BM-derived secretory lineage cells within epithelial cells after the development of GVHD. Another case that developed chronic GVHD also showed a significant increase (0.13 ± 0.075 vs 1.46 ± 0.278 cells/100 epithelial cells, $P = .002$) in the frequency of BM-derived epithelial cells between day 26 (1454 total epithelial cells) and day 161 (1257 total epithelial cells). This was also associated with a substantial increase of BM-derived secretory lineage cells within epithelial cells (0.04 vs 0.68 cells/100 epithelial cells after the development of GVHD). Values are shown as mean ± SE. *Indicates $P < .05$. NS indicates $P \geq .05$.

for terminally differentiated cells within BM-derived epithelial cells. We observed significant differences in the differentiation pattern of BM-derived epithelial cells between GVHD (−) recipients and GVHD (+) recipients with regeneration (Figure 7*A*). BM-derived neuroendocrine cells showed a significant increase (1.0 ± 1.99 vs 12.9 ± 3.78 cells/100 Y-FISH–positive epithelial cells, $P = .002$), whereas BM-derived goblet cells (6.7 ± 2.77 vs 17.2 ± 5.0 cells/100 Y-FISH–positive epithelial cells, $P = .053$) or BM-derived Paneth cells (0.0 ± 0.0 vs 1.1 ± 0.87 cells/100 Y-FISH–positive epithelial cells, $P = .056$) showed a substantial increase in GVHD (+) recipients with regeneration compared with GVHD (−). In sharp contrast, BM-derived absorptive cells showed a significant decrease (79.8 ± 4.61 vs 59.1 ± 9.06 cells/100 Y-FISH–positive epithelial cells, $P = .039$) in GVHD (+) recipients with regeneration compared with GVHD (−). It has recently been proposed that goblet cells, enteroendocrine cells, and Paneth cells arise from a shared progenitor cell and are categorized as secretory lineage cells, which are distinct from absorptive lineage cells.[7,8] Reanalysis of the data in terms of BM-derived secretory lineage cells and BM-derived absorptive lineage cells showed that secretory lineage cells were significantly increased (3.88 ± 1.02, $P = .013$), whereas absorptive lineage cells were significantly decreased (0.74 ± 0.11, $P = .039$) in GVHD (+) recipients with regeneration (Figure 7*B*). Such changes in the lineages of terminally differentiated BM-derived cells were not observed in GVHD (+) recipients without regeneration (secretory lineage cells, 1.75 ± 0.16, $P > .1$; absorptive lineage cells, 0.9 ± 0.19, $P > .1$).

To confirm that BM-derived secretory lineage cells increased during regeneration from GVHD, we further examined series of biopsy specimens taken at different time points from 3 different cases (Figure 7*C*). The first case, which did not develop GVHD (GVHD [−]), showed no increase of BM-derived epithelial cells (0.47 ± 0.154 vs 0.5 ± 0.139 cells/100 epithelial cells, $P > .1$), and the differentiated BM-derived epithelial cells were dominated by absorptive lineage cells. In sharp contrast, the second case, which developed acute GVHD around day 77 post-BMT, showed a significant increase in the total number of BM-derived epithelial cells (0.52 ±0.184 vs 1.56 ± 0.574 cells/100 epithelial cells, $P = .037$) associated with an increase of the secretory lineage cells (0.0 vs 0.571 cells/100 epithelial cells) during regeneration from GVHD. The third case, which developed chronic GVHD, showed the same change as the second case. These results show that BM-derived epithelial cells increase in number via increase of Ki-67–positive cells and, at the same time, generate more BM-derived cells of secretory lineage function in cases of severe intestinal inflammation and the following regeneration of the damaged epithelium. However, in any case, no less than 50% of terminally differentiated BM-derived epithelial cells were absorptive cells. This may be due to the surrounding environment of the small intestine, in which many absorptive cells are required and generated, compared with cells of other lineages.

To examine whether this change in differentiation pattern is unique to BM-derived cells, we examined the differentiation pattern of non–BM-derived cells. Interestingly, the differentiation patterns of both the total epithelial cells (Figure 8*A*) and the Y-FISH–negative epithelial cells (Figure 8*B*) were virtually the same and showed no difference among recipients with GVHD (−), GVHD (+) without regeneration, and GVHD (+) with regeneration. To examine further the contribution of BM-derived cells to the composition of the entire epithelium, we compared the proportions of BM-derived cells in epithelial cells of each lineage. Surprisingly, the proportions of BM-derived goblet cells and neuroendocrine cells were significantly increased in GVHD (+) recipients with regeneration as compared to GVHD (−) recipients (goblet cells, 0.29 ± 0.09 vs 1.39 ± 0.38 cells/100 goblet cells, $P = .006$; neuroendocrine cells, 0.16 ± 0.53 vs 3.95 ± 1.34 cells/100 neuroendocrine cells, $P = .001$), whereas the proportion of BM-derived absorptive cells remained at the same level (Figure 8*C*). The proportion of BM-derived secretory lineage cells was significantly increased (0.24 ± 0.07 vs 1.92 ± 0.51 cells/100 secretory lineage cells, $P = .003$) up to 8-fold in GVHD (+) recipients with regeneration as compared with GVHD (−) recipients. No changes of the proportions of terminally differentiated BM-derived cells were observed in GVHD (+) recipients without regeneration. Collectively, these results suggested that the change in differentiation pattern at the site of intestinal inflammation is unique to BM-derived cells. They also suggested that the proportion of BM-derived secretory lineage cells increases at the site of intestinal inflammation, thereby supporting the specific functions of the epithelium during regeneration from epithelial damage.

Discussion

The present study provides evidence that human BM-derived intestinal epithelial cells are euploid, with only rare cells expressing the stem cell marker Musashi-1 expression and no detectable cells showing the long-term survival thought to be characteristic of stem cells. A few BM-derived cells showed evidence of proliferation,

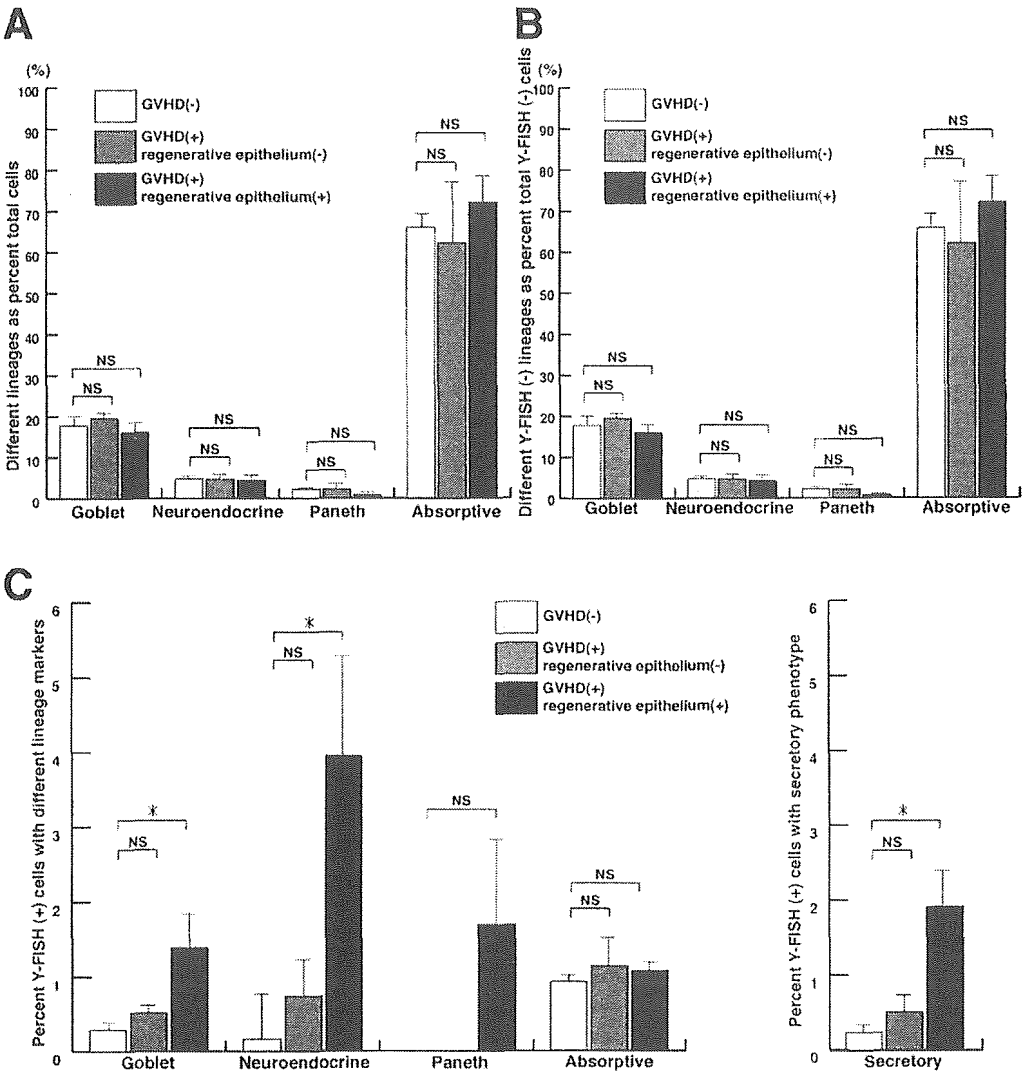

Figure 8. The proportion of BM-derived epithelial cells among total secretory lineage cells increases in the regenerative epithelium following GVHD. (*A*) The differentiation pattern in a total of 30,973 epithelial cells was compared in the 3 groups of patients described in Figure 7*A*. No difference was observed among the groups. Values are shown as mean ± SE. NS indicates $P \geq .05$. (*B*) The differentiation pattern in a total of 30,734 Y-FISH–negative epithelial cells was compared in the 3 groups. No difference was observed among the groups. Values are shown as mean ± SE. NS indicates $P \geq .05$. (*C*) The proportion of BM-derived cells within each lineage was compared in the 3 groups. The proportions of BM-derived goblet cells within total goblet cells and of BM-derived neuroendocrine cells within total neuroendocrine cells were significantly increased in GVHD (+)/regenerative epithelium (+) compared to GVHD (−). Consequently, the proportion of BM-derived secretory lineage cells within total secretory lineage cells was significantly increased up to 8-fold in GVHD (+)/regenerative epithelium (+) compared with GVHD (−), whereas no difference was seen in the proportion of BM-derived absorptive cells. Values are shown as mean ± SE. *Indicates $P < .05$. NS indicates $P \geq .01$.

whereas a majority express markers of terminal differentiation.

Recent studies both in vitro and in vivo have demonstrated that fusion between BM cells and tissue-specific cells could be one mechanism by which BM-derived nonhematopoietic cells arise.[11–15] Cells generated in vivo through this mechanism form polyploid cells called *heterokaryons*, which may subsequently give rise to 2 euploid cells by cytoreductive division.[13,14,27] In the present study using multicolor FISH, no BM-derived epithelial cell examined was found to be a heterokaryon. We have previously reported that no epithelial cell expressing 2 discrete signals of Y-FISH within a single nucleus could be found in the intestinal epithelium of a male BMT recipient whose donor was male.[9] These findings together suggest that BM-derived epithelial cells are euploid cells and not heterokaryons generated by cell fusion. Several reports support the absence or the rare contribution of cell fusion in vivo. A recent report has evaluated cell fusion events in vivo using the Cre/lox system and suggested that epithelial cells of lung, liver, and skin can develop from BM-derived cells without cell fusion.[20] However, our present method cannot exclude the possibility of cell fusion followed by cytoreductive division.

Although several reports have demonstrated the presence of BM-derived epithelial cells within the intestine, it has never been clarified how these cells arise, proliferate, or function within the intestinal epithelium.[9,37–40] In other nonhematopoietic tissues, BM-derived cells are reported to distribute as tissue-specific cells via tissue-specific stem cells[22] or intermediate progenitor cells.[18,41]

Our present results show that BM-derived epithelial cells virtually never express functional or molecular features of intestinal stem cells. On the other hand, we showed that Ki-67–positive, BM-derived epithelial cells occasionally appear to divide at least once within the intestinal epithelium. Moreover, coexpression of various lineage-specific differentiation markers has been frequently observed within BM-derived epithelial cells. Coexpression of these lineage-specific differentiation markers directly reflect the lineage-specific functions of the BM-derived cells, and, thus, we have demonstrated for the first time that BM-derived epithelial cells adopt the specific phenotype of differentiated epithelial cells. However, we did not observe clusters of 3 or more BM-derived epithelial cells, of over 3 adjacent cells, and pairs of BM-derived epithelial cells were rare (3 pairs observed within 30,973 epithelial cells). From these results, we suggest that BM-derived epithelial cells reside as late transit cells with limited dividing potential,[2] which in turn give rise to differentiated, functional epithelial cells within an extremely short period. This is indeed advantageous for the repair of the damaged epithelium because BM-derived cells can immediately function within the epithelium in response to severe tissue injury and thereby support the essential functions of the intestinal epithelium.

A novel finding to emerge from our study is that the proportion of BM-derived epithelial cells expressing markers of secretory lineages increases during epithelial regeneration in response to GVHD. In contrast, the proportion of non-BM-derived, resident epithelial cells expressing markers of secretory lineage did not change during GVHD-associated regeneration. This suggests that, during inflammation and epithelial damage because of GVHD, differentiation of BM-derived epithelial cells toward secretory lineage may be regulated differently compared with resident epithelial cells. This mechanism could have advantages for epithelial repair if the BM-derived secretory lineages express factors such as Trefoil peptides,[42] which promote restitution or mediators of defense such as mucin and antimicrobial peptides. Because Notch signaling[43,44] regulates the decision between secretory and absorptive lineage,[7,45,46] future examination of the expression of this pathway in BM-derived epithelial cells during GVHD and regeneration could be of interest. However, another possibility that BM-absorptive cells have shorter survival time and therefore appear to decrease in relative proportion during inflammation and epithelial damage because of GVHD must also be considered. Effects of inflammatory mediators or mesenchymal cell-derived factors on differentiation of BM-derived epithelial cells to secretory lineage could also be of interest.

In the human intestine, mesenchymal cells such as myofibroblasts are also reported to arise from BM-derived cells and increase their population during regeneration from intestinal inflammation.[47,48] This suggests that both BM-derived epithelial cells and BM-derived mesenchymal cells may share the same origin within the BM cells, such as mesenchymal stem cells. A recent report using a mouse BM transplantation model has suggested that BM-mesenchymal stem cells may be the origin of BM-derived gastrointestinal epithelial cells.[49] However, there are series of studies suggesting hematopoietic stem cells as the origin of BM-derived intestinal epithelial cells.[37,50] Thus, further studies are needed to determine the exact population within BM cells that give rise to BM-derived intestinal epithelial cells or BM-derived mesenchymal cells in the human intestine.[51,52]

In conclusion, BM-derived epithelial cells arise via a mechanism other than cell fusion and virtually never give rise to intestinal stem cells. However, these cells reside as late transit cells, which in turn give rise to differentiated, functional epithelial cells within an extremely short period. During regeneration following epithelial damage, BM-derived cells increase as functional secretory lineage cells, thereby supporting the regeneration and the essential functions of the intestinal epithelium. These results not only provide further evidence for the use of BM-derived cells to regenerate human intestinal epithelium but also suggest the existence of a unique regulatory system targeting BM-derived cells, which can change the differentiation pattern at the site of intestinal inflammation.

References

1. Cheng H, Leblond CP. Origin, differentiation and renewal of the four main epithelial cell types in the mouse small intestine. V. Unitarian theory of the origin of the four epithelial cell types. Am J Anat 1974;141:537–561.
2. Marshman E, Booth C, Potten CS. The intestinal epithelial stem cell. Bioessays 2002;24:91–98.
3. Booth C, Potten CS. Gut instincts: thoughts on intestinal epithelial stem cells. J Clin Invest 2000;105:1493–1499.
4. Bach SP, Renehan AG, Potten CS. Stem cells: the intestinal stem cell as a paradigm. Carcinogenesis 2000;21:469–476.
5. Pinto D, Gregorieff A, Begthel H, Clevers H. Canonical Wnt signals are essential for homeostasis of the intestinal epithelium. Genes Dev 2003;17:1709–1713.
6. Okamoto R, Watanabe M. Molecular and clinical basis for the regeneration of human gastrointestinal epithelia. J Gastroenterol 2004;39:1–6.
7. Yang Q, Bermingham NA, Finegold MJ, Zoghbi HY. Requirement of Math1 for secretory cell lineage commitment in the mouse intestine. Science 2001;294:2155–2158.
8. van Den Brink GR, de Santa Barbara P, Roberts DJ. Development. Epithelial cell differentiation—a Mather of choice. Science 2001; 294:2115–2116.

9. Okamoto R, Yajima T, Yamazaki M, Kanai T, Mukai M, Okamoto S, Ikeda Y, Hibi T, Inazawa J, Watanabe M. Damaged epithelia regenerated by bone marrow-derived cells in the human gastrointestinal tract. Nat Med 2002;8:1011–1017.
10. Okamoto R, Watanabe M. Prospects for regeneration of gastrointestinal epithelia using bone-marrow cells. Trends Mol Med 2003;9:286–290.
11. Ying QL, Nichols J, Evans EP, Smith AG. Changing potency by spontaneous fusion. Nature 2002;416:545–548.
12. Terada N, Hamazaki T, Oka M, Hoki M, Mastalerz DM, Nakano Y, Meyer EM, Morel L, Petersen BE, Scott EW. Bone marrow cells adopt the phenotype of other cells by spontaneous cell fusion. Nature 2002;416:542–545.
13. Wang X, Willenbring H, Akkari Y, Torimaru Y, Foster M, Al-Dhalimy M, Lagasse E, Finegold M, Olson S, Grompe M. Cell fusion is the principal source of bone-marrow-derived hepatocytes. Nature 2003;422:897–901.
14. Vassilopoulos G, Wang PR, Russell DW. Transplanted bone marrow regenerates liver by cell fusion. Nature 2003;422:901–904.
15. Alvarez-Dolado M, Pardal R, Garcia-Verdugo JM, Fike JR, Lee HO, Pfeffer K, Lois C, Morrison SJ, Alvarez-Buylla A. Fusion of bone-marrow-derived cells with Purkinje neurons, cardiomyocytes and hepatocytes. Nature 2003;425:968–973.
16. Tran SD, Pillemer SR, Dutra A, Barrett AJ, Brownstein MJ, Key S, Pak E, Leakan RA, Kingman A, Yamada KM, Baum BJ, Mezey E. Differentiation of human bone marrow-derived cells into buccal epithelial cells in vivo: a molecular analytical study. Lancet 2003; 361:1084–1088.
17. Ianus A, Holz GG, Theise ND, Hussain MA. In vivo derivation of glucose-competent pancreatic endocrine cells from bone marrow without evidence of cell fusion. J Clin Invest 2003;111:843–850.
18. Ferrari G, Cusella-De Angelis G, Coletta M, Paolucci E, Stornaiuolo A, Cossu G, Mavilio F. Muscle regeneration by bone marrow-derived myogenic progenitors. Science 1998;279: 1528–1530.
19. Deb A, Wang S, Skelding KA, Miller D, Simper D, Caplice NM. Bone marrow-derived cardiomyocytes are present in adult human heart: a study of gender-mismatched bone marrow transplantation patients. Circulation 2003;107:1247–1249.
20. Harris RG, Herzog EL, Bruscia EM, Grove JE, Van Arnam JS, Krause DS. Lack of a fusion requirement for development of bone marrow-derived epithelia. Science 2004;305:90–93.
21. Jang YY, Collector MI, Baylin SB, Diehl AM, Sharkis SJ. Hematopoietic stem cells convert into liver cells within days without fusion. Nat Cell Biol 2004;6:532–539.
22. LaBarge MA, Blau HM. Biological progression from adult bone marrow to mononucleate muscle stem cell to multinucleate muscle fiber in response to injury. Cell 2002;111:589–601.
23. Yamada M, Kubo H, Kobayashi S, Ishizawa K, Numasaki M, Ueda S, Suzuki T, Sasaki H. Bone marrow-derived progenitor cells are important for lung repair after lipopolysaccharide-induced lung injury. J Immunol 2004;172:1266–1272.
24. Cooke HJ, Hindley J. Cloning of human satellite III DNA: different components are on different chromosomes. Nucleic Acids Res 1979;6:3177–3197.
25. Devilee P, Slagboom P, Cornelisse CJ, Pearson PL. Sequence heterogeneity within the human alphoid repetitive DNA family. Nucleic Acids Res 1986;14:2059–2073.
26. Nakahori Y, Mitani K, Yamada M, Nakagome Y. A human Y-chromosome specific repeated DNA family (DYZ1) consists of a tandem array of pentanucleotides. Nucleic Acids Res 1986;14: 7569–7580.
27. Weimann JM, Johansson CB, Trejo A, Blau HM. Stable reprogrammed heterokaryons form spontaneously in Purkinje neurons after bone marrow transplant. Nat Cell Biol 2003;5:959–966.
28. Bjerknes M, Cheng H. Clonal analysis of mouse intestinal epithelial progenitors. Gastroenterology 1999;116:7–14.
29. Wright NA. Stem cell repertoire in the intestine. In: Potten CS, ed. Stem cells. 1st ed. London: Academic Press, 2000:315–330.
30. Sakakibara S, Imai T, Hamaguchi K, Okabe M, Aruga J, Nakajima K, Yasutomi D, Nagata T, Kurihara Y, Uesugi S, Miyata T, Ogawa M, Mikoshiba K, Okano H. Mouse-Musashi-1, a neural RNA-binding protein highly enriched in the mammalian CNS stem cell. Dev Biol 1996;176:230–242.
31. Kayahara T, Sawada M, Takaishi S, Fukui H, Seno H, Fukuzawa H, Suzuki K, Hiai H, Kageyama R, Okano H, Chiba T. Candidate markers for stem and early progenitor cells, Musashi-1 and Hes1, are expressed in crypt base columnar cells of mouse small intestine. FEBS Lett 2003;535:131–135.
32. Potten CS, Booth C, Tudor GL, Booth D, Brady G, Hurley P, Ashton G, Clarke R, Sakakibara S, Okano H. Identification of a putative intestinal stem cell and early lineage marker; musashi-1. Differentiation 2003;71:28–41.
33. Nishimura S, Wakabayashi N, Toyoda K, Kashima K, Mitsufuji S. Expression of Musashi-1 in human normal colon crypt cells: a possible stem cell marker of human colon epithelium. Dig Dis Sci 2003;48:1523–1529.
34. Gerdes J, Lemke H, Baisch H, Wacker HH, Schwab U, Stein H. Cell cycle analysis of a cell proliferation-associated human nuclear antigen defined by the monoclonal antibody Ki-67. J Immunol 1984;133:1710–1715.
35. Trejdosiewicz LK, Malizia G, Oakes J, Losowsky MS, Janossy G. Expression of the common acute lymphoblastic leukaemia antigen (CALLA gp100) in the brush border of normal jejunum and jejunum of patients with coeliac disease. J Clin Pathol 1985;38: 1002–1006.
36. Meignin V, Soulier J, Brau F, Lemann M, Gluckman E, Janin A, Socie G. Little evidence of donor-derived epithelial cells in early digestive acute graft versus host disease. Blood 2003;24:24.
37. Krause DS, Theise ND, Collector MI, Henegariu O, Hwang S, Gardner R, Neutzel S, Sharkis SJ. Multi-organ, multi-lineage engraftment by a single bone marrow-derived stem cell. Cell 2001; 105:369–377.
38. Tryphonopoulos P, Icardi M, Salgar S, Ruiz P, Fukumori T, Gandia C, Boukas K, Kato T, Esquenazi V, Ricordi C, Michalopoulos G, Miller J, Tzakis A. Host-derived enterocytes in intestinal grafts. Transplantation 2002;74:120–138.
39. Korbling M, Katz RL, Khanna A, Ruifrok AC, Rondon G, Albitar M, Champlin RE, Estrov Z. Hepatocytes and epithelial cells of donor origin in recipients of peripheral-blood stem cells. N Engl J Med 2002;346:738–746.
40. Spyridonidis A, Schmitt-Graff A, Tomann T, Dwenger A, Follo M, Behringer D, Finke J. Epithelial tissue chimerism after human hematopoietic cell transplantation is a real phenomenon. Am J Pathol 2004;164:1147–1155.
41. Kotton DN, Ma BY, Cardoso WV, Sanderson EA, Summer RS, Williams MC, Fine A. Bone marrow-derived cells as progenitors of lung alveolar epithelium. Development 2001;128:5181–5188.
42. Taupin D, Podolsky DK. Trefoil factors: initiators of mucosal healing. Nat Rev Mol Cell Biol 2003;4:721–732.
43. Schroder N, Gossler A. Expression of Notch pathway components in fetal and adult mouse small intestine. Gene Expr Patterns 2002;2:247–250.
44. Sander GR, Powell BC. Expression of notch receptors and ligands in the adult gut. J Histochem Cytochem 2004;52:509–516.
45. Jensen J, Pedersen EE, Galante P, Hald J, Heller RS, Ishibashi M, Kageyama R, Guillemot F, Serup P, Madsen OD. Control of endodermal endocrine development by Hes-1. Nat Genet 2000; 24:36–44.
46. Wong GT, Manfra D, Poulet FM, Zhang Q, Josien H, Bara T, Engstrom L, Pinzon-Ortiz M, Fine JS, Lee HJ, Zhang L, Higgins GA, Parker EM. Chronic treatment with the γ-secretase inhibitor LY-

411,575 inhibits β-amyloid peptide production and alters lymphopoiesis and intestinal cell differentiation. J Biol Chem 2004;279:12876–12882.
47. Brittan M, Hunt T, Jeffery R, Poulsom R, Forbes SJ, Hodivala-Dilke K, Goldman J, Alison MR, Wright NA. Bone marrow derivation of pericryptal myofibroblasts in the mouse and human small intestine and colon. Gut 2002;50:752–757.
48. Direkze NC, Forbes SJ, Brittan M, Hunt T, Jeffery R, Preston SL, Poulsom R, Hodivala-Dilke K, Alison MR, Wright NA. Multiple organ engraftment by bone-marrow-derived myofibroblasts and fibroblasts in bone-marrow-transplanted mice. Stem Cells 2003; 21:514–520.
49. Houghton J, Stoicov C, Nomura S, Rogers AB, Carlson J, Li H, Cai X, Fox JG, Goldenring JR, Wang TC. Gastric cancer originating from bone marrow-derived cells. Science 2004;306: 1568–1571.
50. Ishikawa F, Yasukawa M, Yoshida S, Nakamura K, Nagatoshi Y, Kanemaru T, Shimoda K, Shimoda S, Miyamoto T, Okamura J, Shultz LD, Harada M. Human cord blood- and bone marrow-derived CD34+ cells regenerate gastrointestinal epithelial cells. FASEB J 2004;18:1958–1960.
51. Herzog EL, Chai L, Krause DS. Plasticity of marrow-derived stem cells. Blood 2003;102:3483–3493.
52. Korbling M, Estrov Z. Adult stem cells for tissue repair: a new therapeutic concept? N Engl J Med 2003;349:570–582.

Received April 3, 2004. Accepted March 9, 2005.

Address requests for reprints to: Mamoru Watanabe, MD, PhD, Department of Gastroenterology and Hepatology, Graduate School Tokyo Medical and Dental University, 1-5-45 Yushima, Bunkyo-ku, Tokyo 113-8519, Japan. e-mail: mamoru.gast@tmd.ac.jp; fax: (81) 3-5803-0262.

Supported in part by grants-in-aid for Scientific Research, Scientific Research on Priority Areas, Exploratory Research, and Creative Scientific Research from the Japanese Ministry of Education, Culture, Sports, Science and Technology; the Japanese Ministry of Health, Labor and Welfare; the Japan Medical Association; Foundation for Advancement of International Science; Terumo Life Science Foundation; Ohyama Health Foundation; Yakult Bio-Science Foundation; and Research Fund of Mitsukoshi Health and Welfare Foundation.

The authors thank Dr. Takaaki Ito for critical comments and Yuko Ito for manuscript preparation.

T.M. and R.O. contributed equally to this study.

Am J Physiol Gastrointest Liver Physiol 288: G745–G754, 2005.
First published November 18, 2004; doi:10.1152/ajpgi.00276.2004.

IL-7 exacerbates chronic colitis with expansion of memory IL-7R^{high} CD4$^+$ mucosal T cells in mice

Eriko Okada,[1,*] Motomi Yamazaki,[1,*] Masanobu Tanabe,[2] Tsutomu Takeuchi,[2] Masanobu Nanno,[3] Shigeru Oshima,[1] Ryuichi Okamoto,[1] Kiichiro Tsuchiya,[1] Tetsuya Nakamura,[1] Takanori Kanai,[1] Toshifumi Hibi,[4] and Mamoru Watanabe[1]

[1]*Department of Gastroenterology and Hepatology, Graduate School, Tokyo Medical and Dental University, Tokyo; Departments of* [2]*Tropical Medicine and Parasitology and* [4]*Internal Medicine, School of Medicine, Keio University, Tokyo; and* [3]*Yakult Central Institute for Microbiological Research, Kunitachi City, Tokyo, Japan*

Submitted 28 June 2004; accepted in final form 15 November 2004

Okada, Eriko, Motomi Yamazaki, Masanobu Tanabe, Tsutomu Takeuchi, Masanobu Nanno, Shigeru Oshima, Ryuichi Okamoto, Kiichiro Tsuchiya, Tetsuya Nakamura, Takanori Kanai, Toshifumi Hibi, and Mamoru Watanabe. IL-7 exacerbates chronic colitis with expansion of memory IL-7R^{high} CD4$^+$ mucosal T cells in mice. *Am J Physiol Gastrointest Liver Physiol* 288: G745–G754, 2005. First published November 18, 2004; doi:10.1152/ajpgi.00276.2004.—We have previously demonstrated that mucosal CD4$^+$ T cells expressing high levels of IL-7 receptor (IL-7R^{high}) are pathogenic cells responsible for chronic colitis. Here we investigate whether IL-7 is directly involved in the expansion of IL-7R^{high} memory CD4$^+$ mucosal T cells and the exacerbation of colitis. We first showed that CD4$^+$ lamina propria lymphocytes (LPLs) from wild-type, T cell receptor-α-deficient (TCR-α$^{-/-}$), and recombinase-activating gene (RAG)-2$^{-/-}$-transferred mice with or without colitis showed phenotypes of memory cells, but only CD4$^+$ LPLs from colitic mice showed IL-7R^{high}. In vitro stimulation by IL-7, but not by IL-15 and thymic stromal lymphopoietin, enhanced significant proliferative responses and survival of colitic CD4$^+$, but not normal CD4$^+$ LPLs. Importantly, in vivo administration of IL-7 mice accelerated the expansion of IL-7R^{high} memory CD4$^+$ LPLs and thereby exacerbated chronic colitis in RAG-2$^{-/-}$ mice transferred with CD4$^+$ LPLs from colitic TCR-α$^{-/-}$ mice. Conversely, the administration of anti-IL-7R monoclonal antibody significantly inhibited the development of TCR-α$^{-/-}$ colitis with decreased expansion of CD4$^+$ LPLs. Collectively, the present data indicate that IL-7 is essential for the expansion of pathogenic memory CD4$^+$ T cells under pathological conditions. Therefore, therapeutic approaches targeting the IL-7R pathway may be feasible in the treatment of human inflammatory bowel disease.

interleukin-7; colitis; memory T cells; lamina propria lymphocytes; proliferation; high-level interleukin-7 receptor

IL-7 IS A PLEIOTROPIC CYTOKINE that is expressed mainly in bone marrow stroma and thymus epithelia (4), although accumulating evidence indicates potential roles of IL-7 in peripheral nonlymphoid tissues as well. We have previously demonstrated that IL-7 is constitutively produced by intestinal epithelial cells and regulates proliferation of lamina propria lymphocytes (LPLs; see Ref. 29). Other investigators demonstrated that IL-7 is crucial for the development of T cell receptor (TCR)-γδ T cells and the formation of Peyer's patches (1, 7, 11, 16) and cryptopatches (8, 26) in mice. These findings indicate that intestinal epithelial cell-derived IL-7 is indispensable for both organization of mucosal lymphoid tissues and regulation of the normal immune response in the intestinal mucosa.

We have also shown a potential role for IL-7/IL-7R-mediated immune responses in intestinal inflammation (30, 31). First, IL-7 transgenic (Tg) mice developed chronic colitis that mimicked histopathological characteristics of human ulcerative colitis (UC). As chronic colitis developed, IL-7 Tg mice showed decreased expression of IL-7 protein in epithelial cells and significant infiltration of CD4$^+$IL-7R$^+$ T cells in the lamina propria. Second, we clarified that mucosal CD4$^+$ T cells expressing high levels of IL-7R (IL-7R^{high}) are the pathogenic T cells that induce chronic colitis and are thus potential targets for treatment of murine chronic colitis (32). We demonstrated that transfer of IL-7R^{high} CD4$^+$ LPLs isolated from colitic mice in immunodeficient mice induces chronic severe colitis. Importantly, the selective elimination of IL-7R^{high} LPLs by administering small amounts of toxin-conjugated anti-IL-7R antibody completely ameliorated ongoing colitis (32). Third, dysregulation of the IL-7/IL-7R system is also observed in colonic mucosa of patients with UC at the active stage (unpublished data).

The mechanism of expansion and survival of IL-7R^{high} CD4$^+$ LPLs in intestinal mucosa is, however, poorly understood. IL-7 is believed to act synergistically with IL-15 to regulate the potential for survival and homeostatic proliferation of memory CD8$^+$ T cells but not memory CD4$^+$ T cells (5, 24, 27), but controversy remains about whether IL-7 itself has a role in supporting the turnover of memory CD4$^+$ T cells. Recent reports indicated that memory CD4$^+$ T cells expressed high levels of IL-7R and responded to IL-7 by prolonged survival in vitro (10, 13, 25). This result indicated that IL-7 has previously unrecognized roles in the regulation of the survival and maintenance in at least a certain subset of memory CD4$^+$ T cells. Especially, it remains unknown whether IL-7 is involved in the dysregulated homeostasis of memory-type pathogenic T cells in autoimmune disorders. Because we have shown that CD4$^+$ LPLs in colitic mice express high levels of IL-7R, we sought to address whether IL-7 contributes to the expansion of those cells under pathogenic autoimmune conditions.

Here we provide evidence that, among LPLs generally exhibiting memory cell phenotypes, only those in mice with

* E. Okada and M. Yamazaki contributed equally to this work.
M. Watanabe, Department of Gastroenterology and Hepatology, Graduate School of Medicine, Tokyo Medical and Dental University, 1-5-45 Yushima, Bunkyo-ku, Tokyo 113-8519, Japan (E-mail: mamoru.gast@tmd.ac.jp).

The costs of publication of this article were defrayed in part by the payment of page charges. The article must therefore be hereby marked "*advertisement*" in accordance with 18 U.S.C. Section 1734 solely to indicate this fact.

American Journal of Physiology – Gastrointestinal and Liver Physiology

chronic colitis express high levels of IL-7R. Stimulation with exogenous recombinant IL-7 (rIL-7) alone in vitro induced significant proliferation of IL-7R^{high} memory CD4$^+$ LPLs isolated from colitic mice but had no effect on that of memory CD4$^+$ LPLs from wild-type (WT) mice. Other epithelial cell-derived cytokines, including IL-15 and thymic stromal lymphopoietin (TSLP), did not induce the proliferation of IL-7R^{high} CD4$^+$ LPLs. Of note, in vivo administration of rIL-7 caused colitis more quickly and in greater severity in mice transferred with CD4$^+$ LPLs from colitic mice. Moreover, inhibition of the IL-7/IL-7R pathway by administration of anti-IL-7R monoclonal antibody (MAb) significantly ameliorated colitis. These data indicate that IL-7 plays a crucial role in expansion of IL-7R^{high} mucosal T cells in memory CD4$^+$ cells and development of chronic colitis. They also suggest that therapeutic approaches targeting this pathway may be feasible in the treatment of human inflammatory bowel disease.

METHODS

Mice. Female C57BL/6 mice were purchased from Japan Clea (Tokyo, Japan). Female TCR-α deficient (TCR-α$^{-/-}$) mice with a background of C57BL/6 were purchased from Jackson Laboratory (Bar Harbor, ME). Female C57BL/6 recombinase-activating gene (RAG)-2-deficient (RAG-2$^{-/-}$) mice were kindly provided by Central Laboratories for Experimental Animals (Kawasaki, Japan). In some experiments, WT littermates were used as controls. Mice used for the transfer colitis experiments were aged 8–12 wk. All mice were maintained in the Animal Care Facility of Tokyo Medical and Dental University. The review board of the University approved the experimental animal studies.

Purification of T cell subsets. Spleens and mesenteric lymph nodes (MLNs) were mechanically dissociated, and the red blood cells were lysed by treatment with 0.84% NH_4Cl. Cells were filtered through a 100-μm-pore-size nylon mesh and suspended in RPMI (Sigma-Aldrich, St. Louis, MO) containing 10% FCS. Splenic CD4$^+$ T cells were isolated from the cell suspension using the anti-CD4 MACS beads system (Miltenyi Biotec, Auburn, CA) according to the manufacturer's instructions. For isolation of colonic LPLs, entire colons were opened longitudinally, washed with PBS, and cut into small (~3 mm) pieces. The dissected specimens were incubated twice with Ca^{2+}- and Mg^{2+}-free Hanks' balanced salt solution containing 1 mM dithiothreitol (GIBCO-BRL, Gaithersburg, MD) for 30 min at 37°C with gentle stirring. The residual tissue fragments were washed and incubated with collagenase A (Roche, Mannheim, Germany) for 2 h at 37°C. The supernatants were collected and washed, and the lymphocyte fraction was isolated on discontinuous Percoll gradients of 75 and 40%. Enriched CD4$^+$ LP T cells were obtained by positive selection using the anti-CD4 MACS magnetic separation system as described above. The resultant cells were shown to contain >96% CD4$^+$ cells by analysis using the FACS Calibur (Becton-Dickinson, Sunnyvale, CA).

Induction of colitis. In this study, the well-characterized CD4$^+$-CD45RB^{high}-induced RAG-2$^{-/-}$ colitis (23) and spontaneous TCR-α$^{-/-}$ colitis (15) models were used. The LP CD4$^+$ T cells isolated from colitic TCR-α$^{-/-}$ (20-wk-old) mice were transferred into RAG-2$^{-/-}$ mice as previously described (32). All animals were weighed, and diarrhea was evaluated as an indicator of colitis.

Flow cytometry. The profiles of spleen, MLN and LP T cells were analyzed by flow cytometry. Cells were preincubated with a F_cγR-blocking MAb (CD16/32; 2.4G2; BD PharMingen, San Diego, CA) for 20 min and then incubated with FITC-, phycoerythrin (PE)-, or biotin-labeled specific antibodies for 30 min on ice. Antibodies used were anti-CD4 MAb (RM4–5; BD PharMingen), anti-TCR-β MAb (H57–597; BD PharMingen), anti-CD25 MAb (HT-2; BD PharMingen), anti-CD44 MAb (IM7; BD PharMingen), anti-CD62L MAb (MEL-14; BD PharMingen), anti-CD69 MAb (H1.2F3; BD PharMingen), and anti-IL-7R MAb (A7R34; kindly provided by Dr. Tetsuo Sudo, Toray Industries, Tokyo, Japan). Biotinylated antibodies were detected with PE-streptavidin (BD PharMingen). Standard two-color flow cytometric analysis was performed using a FACS Caliber (Becton-Dickinson) with the CellQuest software. Staining with isotype-matched control MAbs was performed to assess background fluorescence intensity. Dead cells were eliminated from analysis by 7AAD (BD PharMingen) staining.

Proliferation assay. Splenic (2 × 10^5 cells/well), MLN (1 × 10^5 cells/well) and LP (1 × 10^5 cells/well) CD4$^+$ T cells were seeded on 96-well round microtiter plates and cultured in 10% FCS-containing RPMI, supplemented with 2-mercaptoethanol (GIBCO), penicillin-streptomycin (GIBCO), L-glutamine (GIBCO), and HEPES (GIBCO). After 72 h of incubation, cells were pulsed for 12 h with [^{3}H]thymidine (1 μCi/well), and the [^{3}H]thymidine incorporation was measured with a scintillation counter (Filtermate Harvester; Perkin-Elmer, Boston, MA). Recombinant murine (rm) IL-7 (Peprotech EC, London, UK), rmIL-15 (R&D Systems, Minneapolis, MN), and rmTSLP (R&D Systems) were used for cellular stimulation at concentrations of 0.5–50 ng/ml.

Detection of apoptosis. Isolated colonic CD4$^+$ LPLs resuspended in RPMI 1640 medium supplemented with 10% FCS and 1% penicillin/streptomycin were cultured in 96-well round microtiter plates at 1 × 10^5 cells/well in the absence or presence of rmIL-7 (50 ng/ml). After 10 days of culture, cells were washed with PBS and resuspended in a mixture of 100 μl diluted binding buffer and 5 μl of annexin V-FITC (BD PharMingen) solution, and then 2 μl of 7-amino-actinomysin D were added. After 15 min of incubation at room temperature in the dark, flow cytometry analysis was performed using a FACS Caliber (Becton-Dickinson). A portion of cells was stained with PE-anti-CD4 MAb in parallel, and the percentage of surviving CD4$^+$ cells was determined by evaluating annexin V-negative cells. To analyze Bcl-2 expression in CD4$^+$ LPLs, these cells were cultured in medium supplemented with rIL-7 (50 ng/ml). After 16 h of incubation, cells were fixed and permeabilized with BD Cytofix/Cytoperm solution before intracellular cytokine staining with FITC-conjugated anti-Bcl-2 MAb (3F11; BD PharMingen).

Cytokine assay. To measure cytokine production, isolated CD4$^+$ LPLs were cultured in medium supplemented with 1 μg/ml soluble anti-CD28 MAb (37.51; BD PharMingen) in 96-well plates precoated with 10 μg/ml anti-CD3 MAb (145–2C11; BD PharMingen) in PBS. Culture supernatants were collected, and the cytokine concentrations of IFN-γ, TNF-α, IL-2, IL-4, and IL-5 were determined by flow cytometry with a cytometric bead array set (BD PharMingen) according to the manufacturer's instructions.

Administration of IL-7 in colitic memory IL-7R^{high} CD4$^+$ LPL-transferred RAG-2$^{-/-}$ mice. CD4$^+$ LP T cells were isolated from colitic TCR-α$^{-/-}$ mice (20 wk of age) by use of anti-CD4 MACS beads. The purified CD4$^+$ LPLs (1.5 × 10^5) were intraperitoneally transferred to RAG-2$^{-/-}$ mice. Either rmIL-7 (5 μg/day ip on *days 0–7*) or PBS alone was administered to these mice intraperitoneally, and the effects of IL-7 on the development of colitis were evaluated.

Administration of anti-IL-7R MAb for diseased TCR-α$^{-/-}$ mice. TCR-α$^{-/-}$ mice (8-wk-old) were treated with rat anti-murine IL-7Rα MAb (A7R34) by intraperitoneal injection of a 1-mg dose one time per week for 8 wk. Control mice were treated with the same amounts of purified rat IgG (Sigma-Aldrich). All mice were killed on the day after the last treatment, and colitic lesions were evaluated.

Clinical and histological analysis. Mice were weighed and monitored for appearance and signs of soft stool or diarrhea three times per week. After death, clinical scores were assessed as the sum of the following four parameters: hunching and wasting, 0 or 1; colon thickening, 0–3 (0, no colon thickening; 1, mild thickening; 2, moderate thickening; 3, extensive thickening); and stool consistency, 0–3 (0, normal beaded stool; 1, soft stool; 2, diarrhea; 3, gross bloody stool; see Ref. 9). For histological scoring, the area most affected was

selected and graded by the number and severity of lesions. The mean degree of inflammation in the colon was calculated using a modification of a previously described scoring system (2).

Statistical analysis. The results are expressed as means ± SD. For statistical analysis, we used the program Statview for Macintosh and MS Office (Excel) and analyzed the data by Student's *t*-test.

RESULTS

IL-7R^{high} expression in memory CD4$^+$ LPLs from colitic mice. To determine whether IL-7 directly promotes the expansion of CD4$^+$ T cells in colonic mucosa and the development of chronic colitis, we first investigated the levels of IL-7R expression on CD4$^+$ LPLs in nondiseased (6-wk-old) or diseased TCR-$\alpha^{-/-}$ (18-wk-old) mice, diseased C57BL/6 RAG-2$^{-/-}$ mice reconstituted with CD4$^+$CD45RB^{high} cells for 6 wk, and WT mice (8 wk old). Flow cytometric analysis revealed that the degree of IL-7R expression on CD4$^+$ LPLs from colitic TCR-$\alpha^{-/-}$ mice was significantly higher than that in nondiseased TCR-$\alpha^{-/-}$ or WT mice ($P < 0.01$; Fig. 1*A*). The mean fluorescence intensities (MFI) of IL-7R expression in the flow cytometric histogram were 490 ± 34 in CD4$^+$ LPLs from diseased TCR-$\alpha^{-/-}$ mice, 243 ± 27 from nondiseased TCR-$\alpha^{-/-}$ mice, and 173 ± 37 from WT mice. The degree of IL-7R expression on CD4$^+$ LPLs from colitic RAG-2$^{-/-}$ mice transferred with CD4$^+$CD45RB^{high} cells was also high (MFI: 266 ± 74), but not comparable to the level in CD4$^+$ LPLs from diseased TCR-$\alpha^{-/-}$ mice. In contrast, the expression levels of IL-7R on CD4$^+$ T cells from spleen and MLNs showed no significant differences between the groups (data not shown).

We next assessed CD44, CD62L, and CD45RB expression on CD4$^+$ LPLs from colitic mice and WT mice. All CD4$^+$ LPLs from colitic TCR-$\alpha^{-/-}$ mice, colitic RAG-2$^{-/-}$ mice transferred with CD4$^+$CD45RB^{high} cells and WT mice showed phenotypes of memory cells with CD44^{high}, CD62L^{low}, and CD45RB^{low} (Fig. 1*B*). These results indicate that CD4$^+$ LPLs from all mice show phenotypes of memory cells, but only LPLs in colonic mucosa from colitic mice, especially colitic TCR-$\alpha^{-/-}$ mice, express high levels of IL-7R.

Stimulation with rIL-7 alone in vitro induced expansion and survival of IL-7R^{high} memory CD4$^+$ LPLs isolated from colitic mice. To clarify the mechanism by which CD4$^+$IL-7R^{high} LPLs infiltrated and expanded in the LP, we performed in vitro cell proliferation studies. To determine the effect of IL-7 on CD4$^+$ LPLs from diseased or nondiseased TCR-$\alpha^{-/-}$ mice, diseased CD4$^+$CD45RB^{high} T cell-transferred mice and WT mice were stimulated in vitro with exogenously added rIL-7. Surprisingly, stimulation with rIL-7 alone induced significant increase in DNA synthesis of IL-7R^{high} memory CD4$^+$ LPLs from both types of colitis mice in a concentration-dependent manner (Fig. 2). In sharp contrast, rIL-7 alone did not enhance the proliferation of CD4$^+$ LPLs from WT mice. Interestingly, CD4$^+$ LPLs from diseased TCR-$\alpha^{-/-}$ mice showed higher proliferative responses to rIL-7 than with those from diseased CD4$^+$CD45RB^{high}-transferred mice, reflecting the higher levels of IL-7R expression, as shown in Fig. 1*A*. Consistent with the lower expression of IL-7R on LPLs from nondiseased TCR-$\alpha^{-/-}$ mice (Fig. 1*A*) than that from the paired diseased TCR-$\alpha^{-/-}$ mice, the proliferative responses of LPLs by rIL-7 from nondiseased mice were significantly lower than those from the paired diseased mice (Fig. 2). Furthermore, rIL-7 alone induced a marginal effect on the proliferation of spleen CD4$^+$ cells and MLN CD4$^+$ cells from diseased and nondiseased TCR-$\alpha^{-/-}$ mice or diseased CD4$^+$CD45RB^{high}-transferred mice and WT mice.

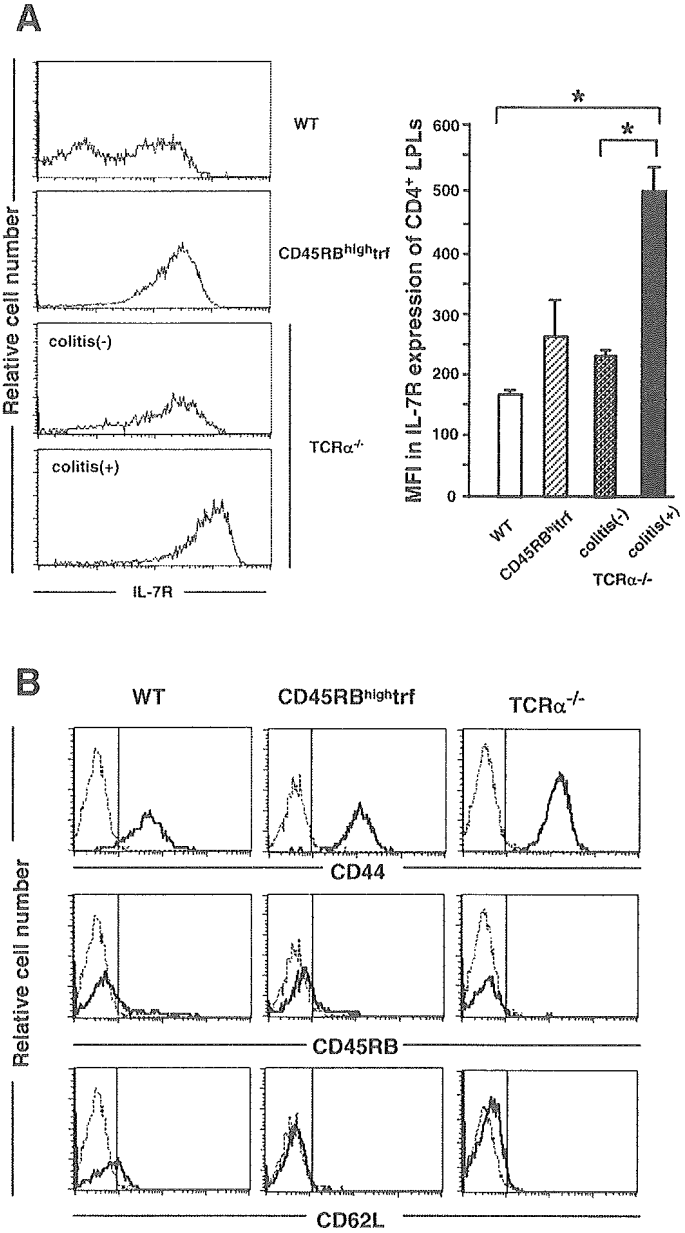

Fig. 1. High-level IL-7 receptor (IL-7R^{high}) expression on memory CD4$^+$ lamina propria lymphocytes (LPLs) from colitic mice. *A*: levels of IL-7R expression on CD4$^+$ LPLs in diseased ($n = 30$) or nondiseased ($n = 9$) T cell receptor-deficient (TCR-$\alpha^{-/-}$) mice, colitic recombinase-activating gene (RAG)-2$^{-/-}$ mice transferred with CD4$^+$CD45RB^{high} cells (CD45RB^{high}trf) ($n = 18$), and wild-type (WT) mice ($n = 32$). The degree of IL-7R expression on CD4$^+$ LPLs from diseased TCR-$\alpha^{-/-}$ mice was significantly (*$P < 0.01$) higher than that in nondiseased TCR-$\alpha^{-/-}$ or WT mice. Mean fluorescence intensity (MFI) of IL-7R expression was 490 ± 34 in CD4$^+$ LPLs from diseased TCR-$\alpha^{-/-}$ mice, 243 ± 27 from nondiseased TCR-$\alpha^{-/-}$ mice, and 173 ± 37 from WT mice. The degree of IL-7R expression on CD4$^+$ LPLs from CD45RB^{high}trf was also high (MFI: 266 ± 74) but not comparable to the level on CD4$^+$ LPLs from colitic TCR-$\alpha^{-/-}$ mice. *B*: CD44, CD62L, and CD45RB expression on CD4$^+$ LPLs from colitic mice and WT mice. CD4$^+$ LPLs from colitic TCR-$\alpha^{-/-}$ mice ($n = 5$), CD45RB^{high}trf ($n = 5$), and WT mice ($n = 8$) all showed phenotypes of memory cells with CD44^{high}, CD62L^{low}, and CD45RB^{low}.

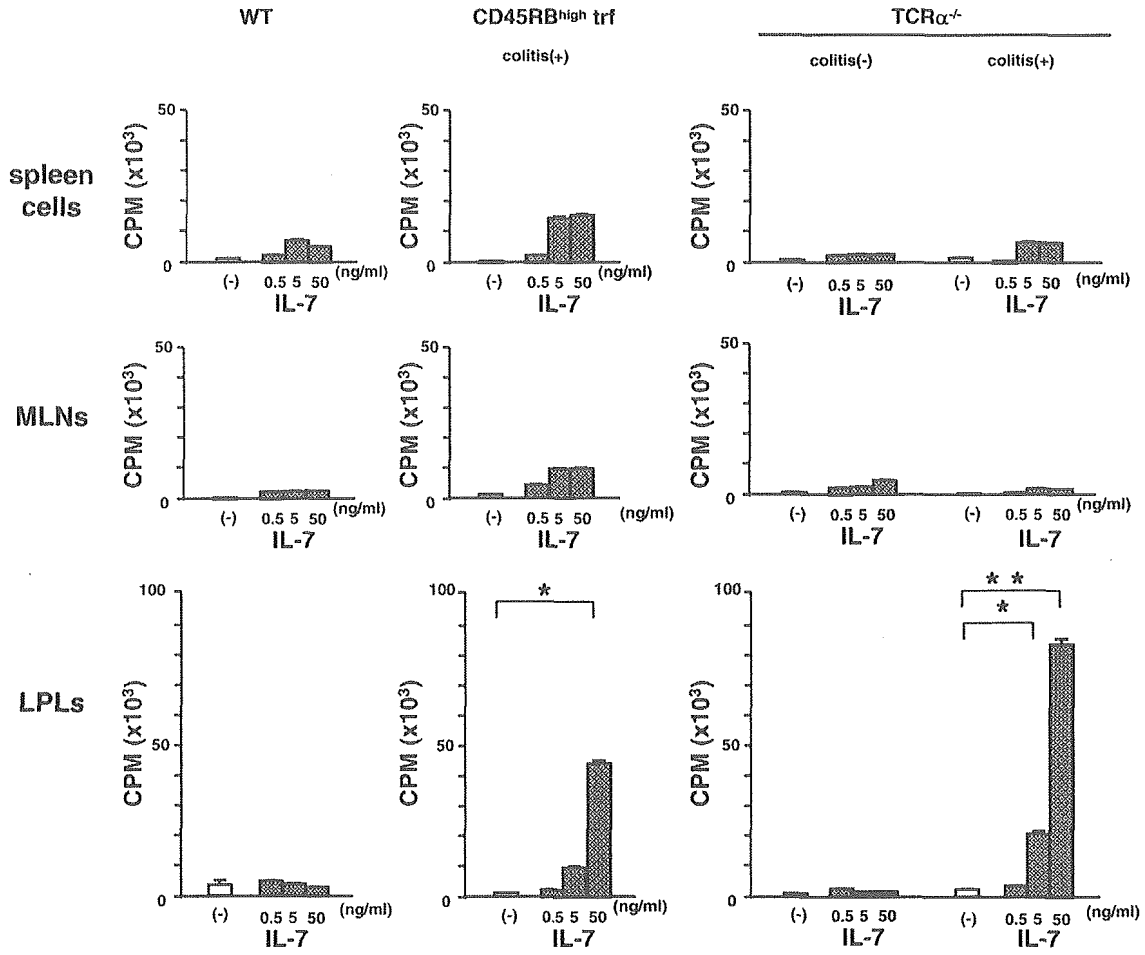

Fig. 2. Stimulation with recombinant (r) IL-7 alone in vitro induced expansion of colitic IL-7R^{high} memory CD4$^+$ LPLs. Stimulation with rIL-7 alone in vitro induced significant increase in DNA synthesis of IL-7R^{high} memory CD4$^+$ LPLs from diseased TCR-$\alpha^{-/-}$ mice (n = 9), but not from nondiseased TCR-$\alpha^{-/-}$ mice (n = 4) or WT mice (n = 16), in a concentration-dependent manner ($^*P < 0.01$, $^{**}P < 0.001$). CD4$^+$ LPLs from colitic CD4$^+$CD45RB^{high}-transferred mice showed smaller proliferative responses to rIL-7 than those from colitic TCR-$\alpha^{-/-}$ mice, reflecting relatively high levels of IL-7R expression (see Fig. 1*A*). rIL-7 alone induced a marginal effect on the proliferation of spleen CD4$^+$ cells and mesenteric lymph node (MLN) cells from diseased or nondiseased TCR-$\alpha^{-/-}$ mice, colitic RAG-2$^{-/-}$ mice transferred with CD4$^+$CD45RB^{high} cells, and WT mice.

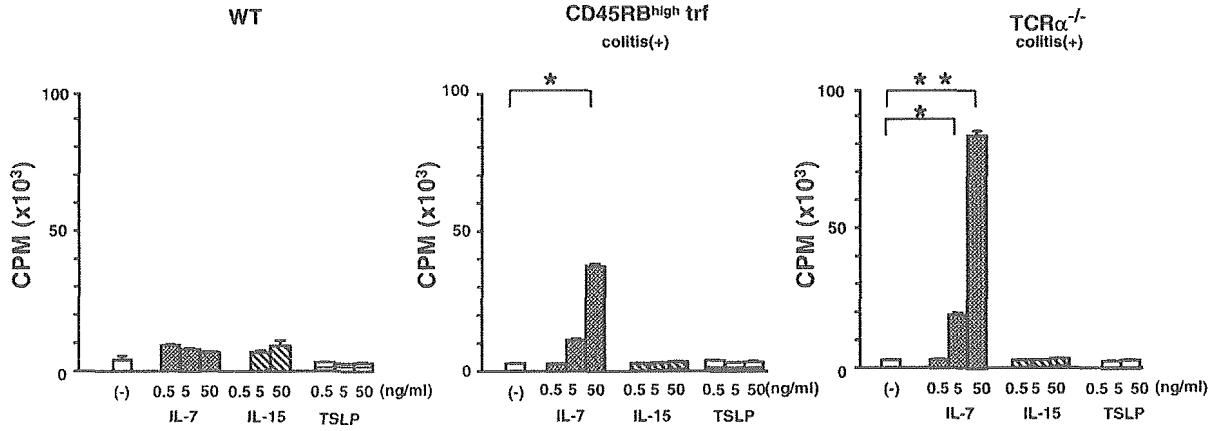

Fig. 3. Effects of different epithelial cell-derived cytokines on the proliferation of the CD4$^+$ LPLs. The responses of CD4$^+$ LPLs to rIL-7, rIL-15, and recombinant thymic stromal lymphopoietin (rTSLP) were compared. rIL-7 alone significantly increased DNA synthesis in CD4$^+$ LPLs from colitic TCR-$\alpha^{-/-}$ mice or colitic CD45RB^{high}-trf mice. In contrast, neither rIL-15 alone nor rTSLP alone could induce the proliferation of CD4$^+$ LPLs from colitic mice or WT mice (n = 5/group).

To further examine whether IL-7 is specifically involved in the proliferative responses of colitic IL-7R^{high}CD4$^+$ LPLs, we assessed the effect of other cytokines secreted by colonic epithelial cells on the proliferation of the CD4$^+$ LPLs. One such factor is IL-15, since previous studies revealed that IL-15 is secreted from intestinal epithelial cells (6) and aberrant production of IL-15 results in chronic colitis (14). Another factor that might induce proliferation of IL-7R^{high}CD4$^+$ LPLs is TSLP. This cytokine shares the IL-7Rα chain with IL-7 (3, 20, 22), and its expression is increased in colitic mucosa from TCR-α$^{-/-}$ mice (data not shown). Thus we compared the proliferative responses of CD4$^+$ LPLs with rIL-7, rIL-15, and rTSLP. Although rIL-7 alone stimulated DNA synthesis in CD4$^+$ LPLs isolated from diseased TCR-α$^{-/-}$ mice or diseased CD4$^+$CD45RB^{high}-transferred mice, neither rIL-15 nor rTSLP could alone induce the proliferative response of CD4$^+$ LPLs from any colitic mice (Fig. 3).

We next tested whether IL-7 promotes the survival of IL-7R^{high} memory CD4$^+$ LPLs isolated from colitic CD4$^+$CD45RB^{high}-transferred mice. As shown in Fig. 4*A*, the number of IL-7R^{high}CD4$^+$ LPLs isolated from colitic mice significantly increased in culture with rIL-7 alone compared with that in culture in the absence of rIL-7. Counts of cultured cells with rIL-7 reached 10-fold of those cultured in the absence of rIL-7. We further examined the apoptosis of those cells in the presence or the absence of rIL-7. After 10 days of culture, >85% of IL-7R^{high}CD4$^+$ LPLs cultured in the presence of rIL-7 were annexin V negative, whereas almost all cells cultured in the absence of rIL-7 were annexin V positive (Fig. 4*B*). To further analyze Bcl-2 expression in CD4$^+$ LPLs simulated with rIL-7, isolated CD4$^+$ LPLs and splenic CD4$^+$ cells from colitic CD45RB^{high}-transferred mice were cultured in medium supplemented with rIL-7 (50 ng/ml). Flow cytometric analysis revealed that the degree of Bcl-2 expression in isolated CD4$^+$ LPLs or splenic CD4$^+$ cells cultured with rIL-7 was upregulated (Fig. 4*C*). All these data raise the possibility that IL-7 promotes both in vitro proliferative expansion and survival of IL-7R^{high}CD4$^+$ memory LPLs that infiltrate the colonic mucosa with chronic colitis.

Because Park and colleagues (21) have recently demonstrated that IL-7 itself suppressed IL-7Rα expression as a novel mechanism for maximizing IL-7-dependent T cell survival, we next evaluated the IL-7R expression on cultured IL-7R^{high}CD4$^+$ LPLs cells with rIL-7. Interestingly, CD4$^+$ LPLs from colitic TCR-α$^{-/-}$ mice, which initially expressed a high level of IL-7R, were significantly downmodulated after the

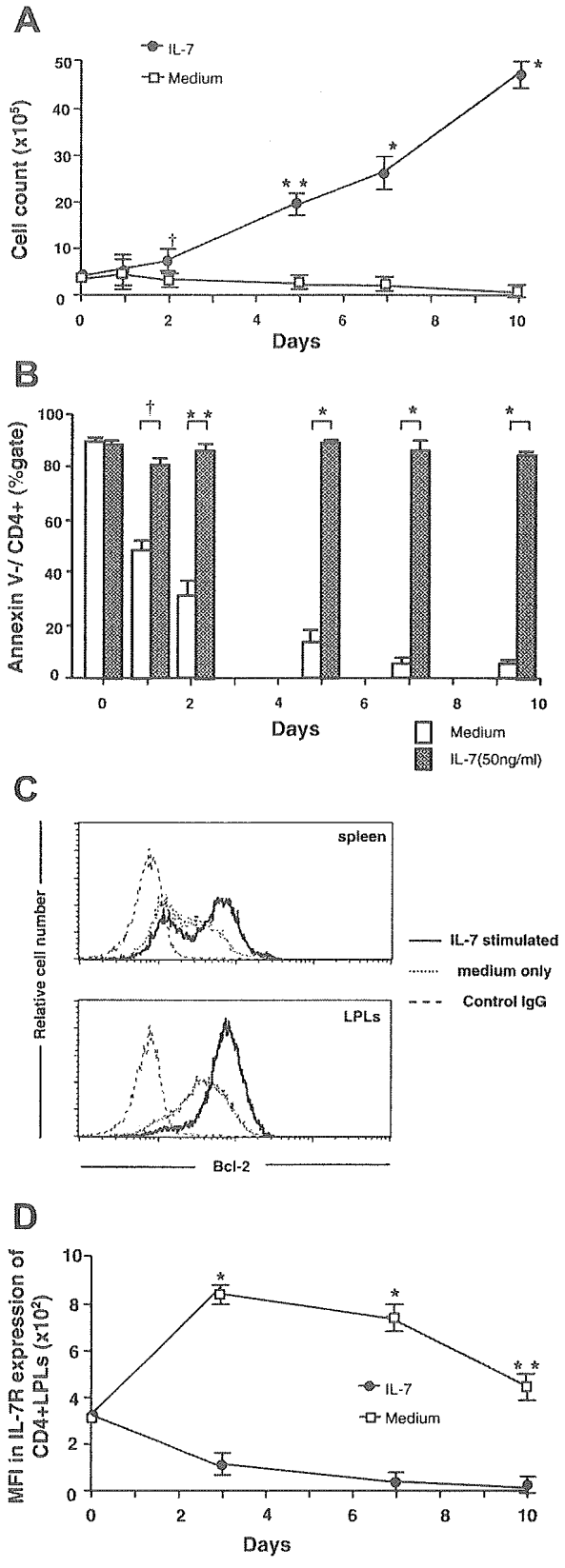

Fig. 4. IL-7 promotes survival in vitro of colitic IL-7R^{high} memory CD4$^+$ LPLs. *A*: no. of IL-7R^{high} CD4$^+$ LPLs isolated from colitic CD45RB^{high}trf mice increased significantly (*$P < 0.0001$, **$P < 0.001$, and †$P < 0.01$) in culture with rIL-7 alone (50 ng/ml), reaching 10-fold the count in culture without rIL-7 ($n = 5$). *B*: IL-7 suppresses apoptosis of colitic IL-7R^{high}CD4$^+$ LPLs. To determine whether rIL-7 increased the survival of memory-phenotype IL-7R^{high} CD4$^+$ LPLs, we examined apoptosis of colitic IL-7R^{high}CD4$^+$ LPLs in the presence or the absence rIL-7 (50 ng/ml). After 10 days of culture, >85% of IL-7R^{high} CD4$^+$ LPLs treated with rIL-7 were annexin V negative, whereas almost all cells cultured in the absence of rIL-7 were annexin V positive (*$P < 0.0001$, **$P < 0.001$, and †$P < 0.01$). *C*: IL-7 upregulated Bcl-2 in colitic IL-7R^{high}CD4$^+$ LPLs. To analyze Bcl-2 expression in CD4$^+$ LPLs simulated with rIL-7, isolated CD4$^+$ LPLs and spleen CD4$^+$ cells from colitic CD45RB^{high}trf mice were cultured with rIL-7 (50 ng/ml). Flow cytometric analysis revealed that the degree of Bcl-2 expression was substantially increased after stimulation with rIL-7 in CD4$^+$ LPLs from colitic mice. *D*: IL-7R expression on cultured IL-7R^{high}CD4$^+$ LPLs with rIL-7. CD4$^+$ LPLs from colitic TCR-α$^{-/-}$ mice, which initially expressed a high level of IL-7R, were significantly (*$P < 0.001$ and **$P < 0.01$) downmodulated after the culture with rIL-7 compared with those cultured without rIL-7.

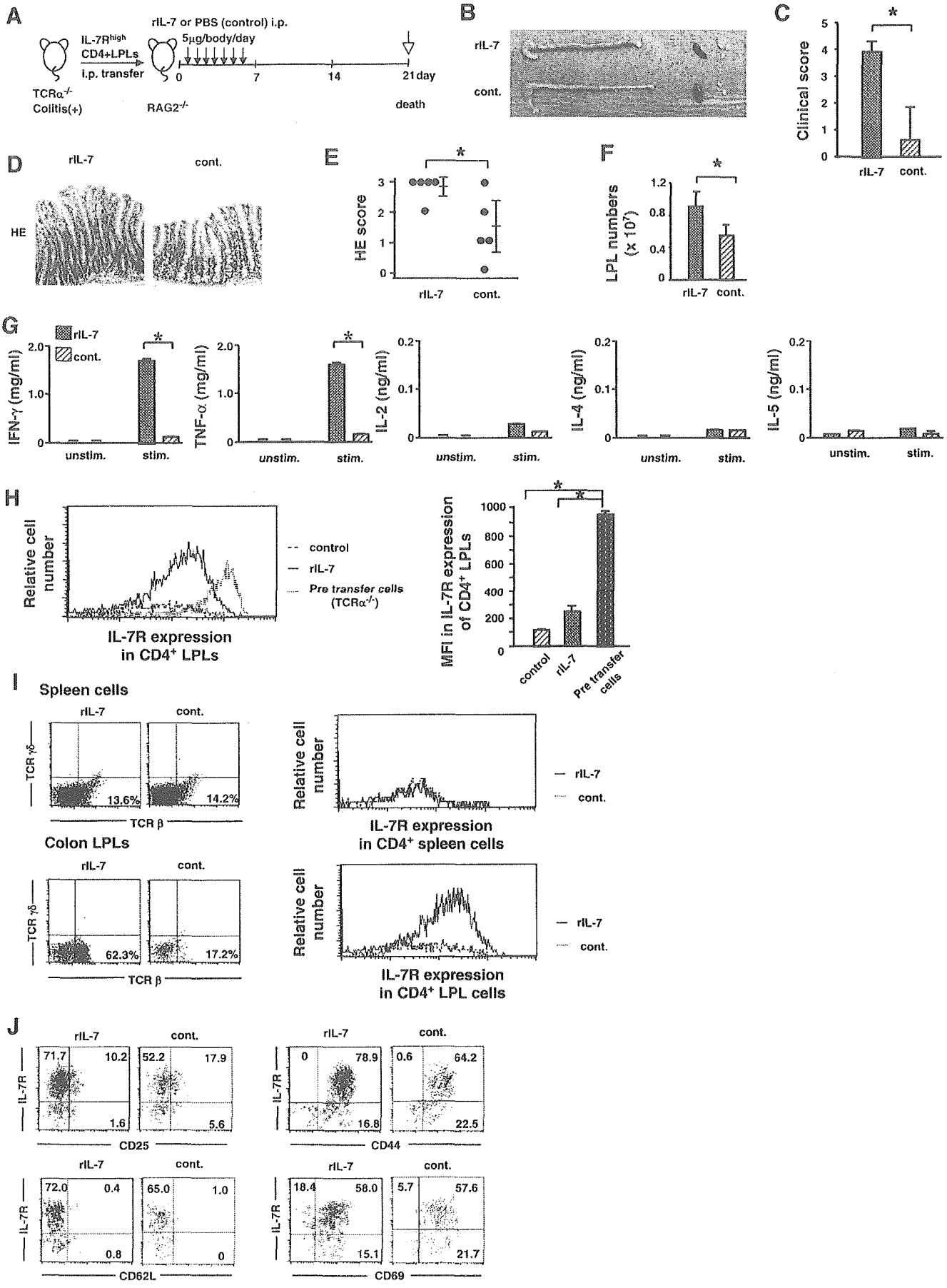

culture with rIL-7 compared with those cultured without rIL-7 (Fig. 4*D*).

In vivo administration of IL-7 exacerbates colitis in RAG-2$^{-/-}$ mice transferred with IL-7R^{high}CD4^{+} TCR-α$^{-/-}$ LPLs. To assess whether the enhancing effect of IL-7 on the expansion of IL-7R^{high}CD4^{+} LPLs in vitro is likewise observed in vivo, we tested whether in vivo rIL-7 administration might influence the colonic inflammation-induced RAG-2$^{-/-}$ mice transferred with IL-7R^{high}CD4^{+} LPLs isolated from colitic TCR-α$^{-/-}$ mice (Fig. 5*A*). Our previous studies showed that recipient mice transferred with 1.5×10^5 IL-7R^{high} CD4^{+} LPLs from colitic TCR-α$^{-/-}$ mice developed colitis within 6 wk after the transfer. rIL-7 was intraperitoneally injected in those recipient mice daily on *days 0–7* after the cell transfer. Intriguingly, IL-7-treated recipient mice, but not PBS-treated mice, rapidly showed severe weight loss and wasting disease at 2–3 wk after the transfer, and we killed all recipient mice at 3 wk after the transfer.

At 3 wk after the transfer, gross inspection of the colon in recipient mice treated with rIL-7 revealed increased inflammatory activity compared with the PBS-injected control group (Fig. 5*B*). Moreover, the clinical score of mice treated with rIL-7 was significantly ($P < 0.01$) higher than that of PBS-treated controls (Fig. 5*C*). Histological analysis of colonic mucosa showed development of severe colitis in recipient mice treated with rIL-7 (Fig. 5*D*). In contrast, mice treated with PBS alone developed only mild colitis at 3 wk after the transfer. As expected, the histological score assessing the severity of inflammation was significantly ($P < 0.05$) increased in mice treated with rIL-7 compared with PBS-injected mice (Fig. 5*E*). Total cell numbers of isolated colonic LPLs were significantly ($P < 0.05$) increased in mice treated with rIL-7 administration (Fig. 5*F*). These results indicate that rIL-7 administration has an escalating effect on the onset of colitis in RAG-2$^{-/-}$ mice transferred with IL-7R^{high}CD4^{+} memory TCR-α$^{-/-}$ T cells.

Cytokine production of isolated CD4^{+} LPLs in RAG-2$^{-/-}$ mice after stimulation with anti-CD3 MAb and anti-CD28 MAb were quite different. Isolated CD4^{+} LPLs from mice treated with rIL-7 produced significantly higher amounts of IFN-γ ($P < 0.001$) and TNF-α ($P < 0.001$), but not IL-2, IL-4, and IL-5 ($P < 0.05$), compared with those from PBS-treated mice (Fig. 5*G*).

Interestingly, flow cytometric analysis revealed that the degree of IL-7R expression in isolated CD4^{+} LPLs of recipient mice treated with rIL-7 or PBS was significantly decreased compared with that in freshly isolated CD4^{+} LPLs from colitic TCR-α$^{-/-}$ mice but still higher than that on normal CD4^{+} LPLs (Fig. 5*H*). In CD4^{+} LPLs of recipient mice treated with rIL-7, TCR-β^{dim} cells were significantly increased and IL-7R expression on CD4^{+} LPLs was higher than that in spleen CD4^{+} cells (Fig. 5*I*). In contrast, the expression of IL-7R on LPLs from WT mice was much lower than that in mice treated with rIL-7. These infiltrated CD4^{+}IL-7R^{high} LPLs from rIL-7-treated recipient mice with severe colitis mainly consisted of memory cells with CD44^{high}, CD62L^{low}, and CD45RB^{low} (Fig. 5*J*). Collectively, these data indicate that in vivo administration of rIL-7 worsens chronic colitis, probably through the expansion of memory CD4^{+} LPLs in RAG-2$^{-/-}$ mice transferred with LPLs from colitic mice.

Blockade of the IL-7/IL-7R pathway ameliorated colitis with decrease of memory CD4^{+} LPLs. To prove the role of IL-7 in the exacerbation of chronic colitis with expansion of IL-7R^{high} LPLs, we finally attempted to control chronic colitis by inhibiting the IL-7/IL-7R pathway using a blocking antibody-based strategy. We found that 50 μg/ml of anti-IL-7R MAb used in this assay efficiently inhibited in vitro proliferation of CD4^{+} LPLs from chronically inflamed mucosa of TCR-α$^{-/-}$ mice (data not shown). In this setting, we used established TCR-α$^{-/-}$ mice rather than the above-mentioned RAG-2$^{-/-}$ mice reconstituted with CD4^{+}IL-7R^{high} memory T cells, with the scope of clinical application to human inflammatory bowel disease. Because TCR-α$^{-/-}$ mice were shown to develop colitis at 12–16 wk of age in our breeding laboratory, we started the treatment at 8 wk of age. We diagnosed these mice by observing weight loss, ruffle appearance, signs of soft stool and diarrhea. We treated chronic colitis in TCR-α$^{-/-}$ mice by intraperitoneal injection of 1 mg anti-IL-7R MAb weekly for 8 wk (Fig. 6*A*). Blockade of the IL-7/IL-7R pathway by anti-IL-7R MAb significantly ameliorated the development of chronic colitis in TCR-α$^{-/-}$ mice. In clear contrast, TCR-α$^{-/-}$ mice treated in parallel with an isotype-matched control antibody developed severe colitis, as shown by diarrhea, bloody stool, and weight loss. Gross inspection and histological analysis of the colon in anti-IL-7R MAb-treated TCR-α$^{-/-}$ mice revealed marked reduction in the inflammatory activity (Fig. 6*B*). This difference was confirmed by histological scoring of multiple colon sections, which gave scores of 1.33 ± 0.21 in anti-IL-7R MAb-treated mice vs. 2.67 ± 0.21 in control rat IgG-treated mice ($P < 0.01$; Fig. 6*C*). In addition, the number of CD4^{+} LPLs was significantly decreased in mice treated with anti-IL-7R MAb (Fig. 6*D*). These results indicate that blockade of the IL-7/IL-7R pathway leads to inhibition of chronic colitis with decreased memory CD4^{+} LPLs.

DISCUSSION

The most important findings of the present study were that exogenously added IL-7 directly promoted the expansion and

Fig. 5. In vivo administration of rIL-7 exacerbated colitis in RAG-2$^{-/-}$ mice transferred with IL-7R^{high}CD4^{+} TCR-α$^{-/-}$ LPLs. *A*: experimental protocol. RAG-2$^{-/-}$ mice were injected ip with IL-7R^{high}CD4^{+} LPLs (1.5×10^5) from colitic TCR-α$^{-/-}$ mice. rIL-7 (5 μg/body) or PBS was injected ip every day on *days 0–7* after the transfer. All mice (n = 5/group) were killed at 3 wk after the transfer. *B*: gross inspection of the colon in mice treated with rIL-7 revealed increased inflammation compared with the PBS-treated control (cont) group. *C*: clinical score of mice treated with rIL-7 was significantly (*$P < 0.01$) higher than that of PBS-treated mice. *D*: hematoxylin and eosin (HE) staining of colonic mucosa showed more severe colitis in mice treated with rIL-7. Magnification: ×100. *E*: histological scores. *$P < 0.01$. *F*: total cell numbers of isolated LPLs. Cell number of LPLs from mice treated with rIL-7 was significantly (*$P < 0.05$) increased compared with that from PBS-treated mice. *G*: cytokine production of isolated CD4^{+} LPLs. Isolated CD4^{+} LPLs from mice treated with rIL-7 produced significantly higher amounts of IFN-γ (*$P < 0.001$) and TNF-α (*$P < 0.001$) than those from PBS-treated mice. *H*: flow cytometric analysis revealed that the degree of IL-7R expression in isolated CD4^{+} LPLs from mice treated with rIL-7 was significantly downregulated compared with that in LPLs from PBS-treated mice. *I*: TCR-β^{dim} LPLs, but not splenocytes, were markedly increased in IL-7-treated mice compared with those in PBS-treated mice. IL-7R expression on CD4^{+} LPLs was still higher than that in splenic CD4^{+} cells. *J*: infiltrated LPLs from rIL-7-treated mice mainly consisted of IL-7R^{high} memory CD4^{+} cells with CD44^{high}, CD62L^{low}, and CD45RB^{low}.

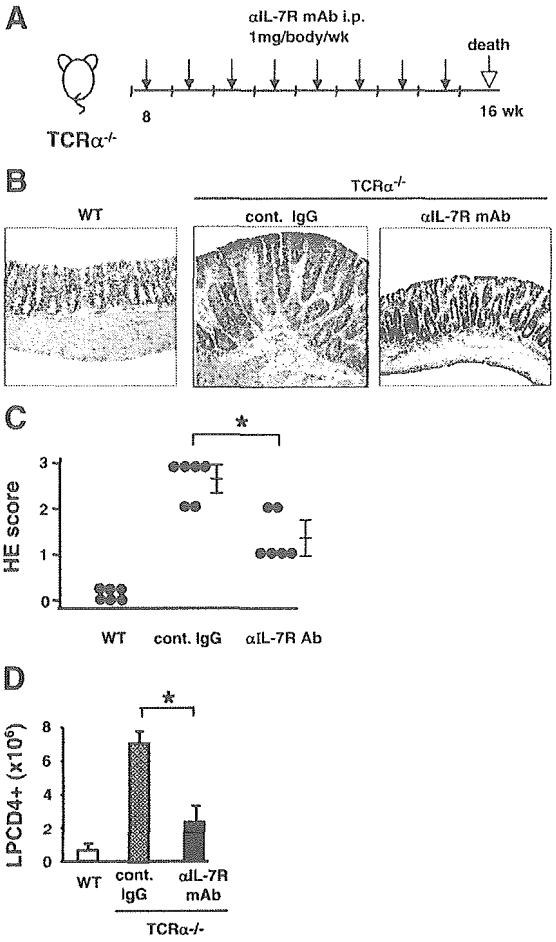

Fig. 6. Blockade of IL-7-IL-7R pathway ameliorated colitis with decrease of memory CD4$^+$ LPLs. *A*: experimental protocol. TCR-$\alpha^{-/-}$ mice (8 wk-old) were treated by ip injection of the anti-IL-7R monoclonal antibody (MAb; 1 mg/body) or isotype-matched control IgG (1 mg/body) one time per week for 8 wk (n = 6, each group). *B*: histological analysis of the colon in anti-IL-7R MAb-treated TCR-$\alpha^{-/-}$ mice revealed marked reduction in the inflammatory activity. In striking contrast, TCR-$\alpha^{-/-}$ mice treated in parallel with control antibody developed severe colitis. *C*: histological scores of colitis in control IgG-treated mice and anti-IL-7R-treated mice. Data are means ± SE of 6 mice in each group. Ab, antibody. *$P < 0.01$. *D*: total cell numbers of isolated LPLs. The number of CD4$^+$ LPLs was significantly (*$P < 0.05$) decreased in TCR-$\alpha^{-/-}$ mice treated with anti-IL-7R MAb.

the survival of IL-7R^{high} memory CD4$^+$ LPLs in vitro and the exacerbation of chronic colitis in vivo. This is the first report that IL-7 mediates the expansion and maintenance of IL-7R^{high} memory CD4$^+$ T cells under pathological colitic conditions.

We have previously demonstrated the potential roles of the IL-7-IL-7R pathway in intestinal inflammation in a series of studies. First, we showed that IL-7 Tg mice developed chronic colitis that mimicked histopathological characteristics of UC in humans (30). In the colonic mucosa of colitic IL-7 Tg mice, marked infiltration of IL-7R^{high} LPLs was demonstrable. Second, we demonstrated that IL-7R^{high}CD4$^+$ LPLs in colitic TCR-$\alpha^{-/-}$ mice were pathogenic, because immunodeficient mice in which these cells were transferred developed similar colitis. Third, we showed that these IL-7R^{high} LPLs are potential targets for the treatment of chronic colitis (32). In RAG-2$^{-/-}$ mice transferred with colitic TCR-$\alpha^{-/-}$ LPLs, the expansion of transferred IL-7R^{high}CD4$^+$ LPLs reached 100 times the colitic mucosa of recipient mice, and their selective elimination by small amounts of toxin-conjugated anti-IL-7Rα antibody completely ameliorated ongoing colitis (32). The reason for the substantial proliferative response of the IL-7R^{high}CD4$^+$ LPLs remains unclear, because IL-7 production in the epithelial cells was conversely decreased according to goblet depletion (unpublished observations). Recent studies have indicated that IL-7 is implicated in the survival and homeostatic proliferation of naive CD4$^+$ T cells (12, 24, 27, 28). It was also demonstrated that IL-7 could have previously unrecognized roles in the survival and generation of memory CD4$^+$ cells (10, 13, 25). For instance, low doses of IL-7 serve as a survival factor for effector memory CD4$^+$ cells, and high doses of IL-7 induce proliferation of memory cells (13). IL-7 directly regulates both survival and expansion of memory CD4$^+$ cells (10, 13, 25). Kondrack et al. (10) demonstrated that memory CD4$^+$ cells expressing comparable levels of IL-7R to naive T cells show sustained cellular survival in response to IL-7 in vivo. Thus IL-7 would be a good candidate for proliferation and survival of colitogenic IL-7R^{high}CD4$^+$ memory LPLs. In the current study, we demonstrated that in vitro stimulation with IL-7, but not IL-15 and TSLP, induced a proliferative response in IL-7R^{high}CD4$^+$ LPLs from colitic TCR-$\alpha^{-/-}$ mice or colitic CD4$^+$CD45RB^{high} T cell-transferred mice. In sharp contrast, memory CD4$^+$ LPLs from nondiseased TCR-$\alpha^{-/-}$ mice or WT mice did not respond to IL-7. Interestingly, CD4$^+$ LPLs from colitic TCR-$\alpha^{-/-}$ mice showed more potent ability to proliferate than those from colitic CD4$^+$CD45RB^{high}-transferred mice, suggesting that the proliferation response on IL-7 stimulation depends on the expression levels of IL-7R. However, the possibility cannot be excluded that reactivities to IL-7 are dependent on the Th2-dominant (TCR-$\alpha^{-/-}$ mice) or Th1-dominant (CD4$^+$CD45RB^{high}-transferred mice) immune model. Upon continuous in vitro stimulation with IL-7, colitic CD4$^+$ LPLs survived and expanded for 10 days in this study (Fig. 4*D*), and actually survived for several weeks in the following study (unpublished observation). These data indicate that IL-7 promotes both expansion and survival in vitro of IL-7R^{high} memory CD4$^+$ LPLs that infiltrated the colonic mucosa with chronic colitis.

In the present study, we also demonstrated that in vivo administration of IL-7 worsened chronic colitis with expansion of IL-7R^{high} memory CD4$^+$ LPLs in RAG-2$^{-/-}$ mice transferred with those LPLs from colitic TCR-$\alpha^{-/-}$ mice. Moreover, blockade of IL-7R by an antibody-based strategy in vivo led to inhibition of colitis with decreased memory CD4$^+$ LPLs. Therefore, we conclude that IL-7 itself plays crucial roles in the expansion of IL-7R^{high} memory CD4$^+$ mucosal T cells and exacerbation of chronic colitis, although it is also possible that yet-unknown cytokines are involved in this mechanism.

We have recently demonstrated that intestinal epithelial cells also express IL-7R and that bone marrow-derived epithelial cells can differentiate into the epithelium of the gastrointestinal tract in humans (18, 19). Epithelial cells of male donor origin were distributed throughout the entire gastrointestinal tract of female bone marrow transplant recipients. Donor-derived epithelial cells remarkably repopulated the gastrointestinal tract during epithelial regeneration. Therefore, we suggest that the IL-7-IL-7R pathway may have previously unrecognized roles in the mucosal immune system.

Surprisingly, however, we found that IL-7R expression on IL-7-stimulated IL-7R^{high}CD4$^+$ LPLs was significantly down-modulated compared with that on freshly isolated IL-7R^{high}CD4$^+$ LPLs in vitro. Similarly, Park and colleagues (21) very recently demonstrated a novel regulatory mechanism that specifically suppressed IL-7Rα expression on normal murine T cells in response to IL-7. Furthermore, we have previously demonstrated that IL-7 expression in colonic epithelial cells is decreased in colonic mucosa with murine chronic colitis, such as IL-7 Tg mice and TCR-α$^{-/-}$ mice (30). Therefore, we assessed the effect of other cytokines, such as IL-15 and TSLP, secreted by colonic epithelial cells on the expansion of IL-7R^{high} memory CD4$^+$ LPLs in chronic colitic lesions. Our results revealed that neither IL-15 nor TSLP alone induced the proliferation of IL-7R^{high} memory CD4$^+$ LPLs from colitic mice or IL-7R^{low} memory CD4$^+$ LPLs from WT mice. Collectively, these results indicate that IL-7 from a source outside the intestine or yet-unknown cytokines may be responsible for the proliferation of IL-7R^{high}CD4$^+$ LPLs on colitic mucosa. Consistent with this hypothesis, a recent report has shown that serum concentration of IL-7 is strongly upregulated, and IL-7 is produced by dendritic-like cells within peripheral lymphoid tissues in human immunodeficiency virus-infected patients (17). Furthermore, it is also possible that colitogenic IL-7 highly sensitive IL-7R^{high} CD4$^+$ LPLs can sufficiently respond to decreased IL-7 in the inflamed mucosa, although the mechanism of the sustained IL-7R^{high} expression on pathogenic CD4$^+$ LPLs remains largely unclear. Further study will be needed to address this issue.

We have some evidence that the IL-7-IL-7R pathway in the colonic mucosa is disturbed in human UC (unpublished observation). Human inflammatory bowel disease is thought to result from inappropriate activation of the mucosal immune system driven by luminal antigens. The activation of important cell populations is eventually accompanied by the production of a wide variety of nonspecific mediators of inflammation. including many other inflammatory and proinflammatory cytokines, chemokines, and growth factors. We suggest that IL-7R^{high} memory CD4$^+$ LPLs are one such important cell population. Therefore, this study provides a basis for practical application of therapy targeting the IL-7-IL-7R pathway for the treatment of chronic intestinal inflammation in human inflammatory bowel disease.

ACKNOWLEDGMENTS

We thank Hiroshi Kiyono and Hiromichi Ishikawa for helpful discussion, Drs. Tatsuji Nomura and Kenichi Tamaoki for providing RAG-2$^{-/-}$ mice, Dr. Masami Moriyama for providing rIL-7, Dr. Tetsuo Sudo for providing anti-IL-7R MAb, Dr. Shin-ichiro Shimad and Noriko Nagaoka for providing TCR-α$^{-/-}$ mice, and Yuko Ito for manuscript preparation.

GRANTS

This study was supported in part by grants-in-aid for Scientific Research, Scientific Research on Priority Areas, Exploratory Research, and Creative Scientific Research from the Japanese Ministry of Education, Culture, Sports, Science and Technology; the Japanese Ministry of Health, Labor, and Welfare; the Japan Medical Association; Foundation for Advancement of International Science; Terumo Life science Foundation; Ohyama Health Foundation; Yakult Bio-Science Foundation; Research Fund of Mitsukoshi Health and Welfare Foundation.

REFERENCES

1. **Adachi S, Yoshida H, Honda K, Maki K, Saijo K, Ikuta K, Saito T, and Nishikawa SI.** Essential role of IL-7 receptor alpha in the formation of Peyer's patch anlage. *Int Immunol* 10: 1–6, 1998.
2. **De Jong YP, Comiskey M, Kalled SL, Mizoguchi E, Flavell RA, Bhan AK, and Terhorst C.** Chronic murine colitis is dependent on the CD154/CD40 pathway and can be attenuated by anti-CD154 administration. *Gastroenterology* 119: 715–723, 2000.
3. **Friend SL, Hosier S, Nelson A, Foxworthe D, Williams DE, and Farr A.** A thymic stromal cell line supports in vitro development of surface IgM+ B cells and produces a novel growth factor affecting B and T lineage cells. *Exp Hematol* 22: 321–328, 1994.
4. **Fry TJ and Mackall CL.** Interleukin-7: from bench to clinic. *Blood* 99: 3892–3904, 2002.
5. **Goldrath AW, Sivakumar PV, Glaccum M, Kennedy MK, Bevan MJ, Benoist C, Mathis D, and Butz EA.** Cytokine requirements for acute and Basal homeostatic proliferation of naive and memory CD8+ T cells. *J Exp Med* 195: 1515–1522, 2002.
6. **Grabstein KH, Eisenman J, Shanebeck K, Rauch C, Srinivasan S, Fung V, Beers C, Richardson J, Schoenborn MA, Ahdieh M, Johnson L, Alderson MR, Watson JD, Anderson DM, and Giri JG.** Cloning of a T cell growth factor that interacts with the beta chain of the interleukin-2 receptor. *Science* 264: 965–968, 1994.
7. **He YW and Malek TR.** Interleukin-7 receptor alpha is essential for the development of gamma delta + T cells, but not natural killer cells. *J Exp Med* 184: 289–293, 1996.
8. **Kanamori Y, Ishimaru K, Nanno M, Maki K, Ikuta K, Nariuchi H, and Ishikawa H.** Identification of novel lymphoid tissues in murine intestinal mucosa where clusters of c-kit+ IL-7R+ Thy1+ lympho-hemopoietic progenitors develop. *J Exp Med* 184: 1449–1459, 1996.
9. **Kinoshita N, Hiroi T, Ohta N, Fukuyama S, Park EJ, and Kiyono H.** Autocrine IL-15 mediates intestinal epithelial cell death via the activation of neighboring intraepithelial NK cells. *J Immunol* 169: 6187–6192, 2002.
10. **Kondrack RM, Harbertson J, Tan JT, McBreen ME, Surh CD, and Bradley LM.** Interleukin 7 regulates the survival and generation of memory CD4 cells. *J Exp Med* 198: 1797–1806, 2003.
11. **Laky K, Lefrancois L, Lingenheld EG, Ishikawa H, Lewis JM, Olson S, Suzuki K, Tigelaar RE, and Puddington L.** Enterocyte expression of interleukin 7 induces development of gammadelta T cells and Peyer's patches. *J Exp Med* 191: 1569–1580, 2000.
12. **Lantz O, Grandjean I, Matzinger P, and Di Santo JP.** Gamma chain required for naive CD4+ T cell survival but not for antigen proliferation. *Nat Immun* 1: 54–58, 2000.
13. **Li J, Huston G, and Swain SL.** IL-7 promotes the transition of CD4 effectors to persistent memory cells. *J Exp Med* 198: 1807–1815, 2003.
14. **Liu Z, Geboes K, Colpaert S, D'Haens GR, Rutgeerts P, and Ceuppens JL.** IL-15 is highly expressed in inflammatory bowel disease and regulates local T cell-dependent cytokine production. *J Immunol* 164: 3608–3615, 2000.
15. **Mombaerts P, Mizoguchi E, Grusby MJ, Glimcher LH, Bhan AK, and Tonegawa S.** Spontaneous development of inflammatory bowel disease in T cell receptor mutant mice. *Cell* 75: 274–282, 1993.
16. **Moore TA, von Freeden-Jeffry U, Murray R, and Zlotnik A.** Inhibition of gamma delta T cell development and early thymocyte maturation in IL-7 -/- mice. *J Immunol* 157: 2366–2373, 1996.
17. **Napolitano LA, Grant RM, Deeks SG, Schmidt D, De Rosa SC, Herzenberg LA, Herndier BG, Andersson J, and McCune JM.** Increased production of IL-7 accompanies HIV-1-mediated T-cell depletion: implications for T-cell homeostasis. *Nat Med* 7: 73–79, 2001.
18. **Okamoto R and Watanabe M.** Prospects for regeneration of gastrointestinal epithelia using bone-marrow cells. *Trends Mol Med* 9: 286–290, 2003.
19. **Okamoto R, Yajima T, Yamazaki M, Kanai T, Mukai M, Okamoto S, Ikeda Y, Hibi T, Inazawa J, and Watanabe M.** Damaged epithelia regenerated by bone marrow-derived cells in the human gastrointestinal tract. *Nat Med* 8: 1011–1017, 2002.
20. **Pandey A, Ozaki K, Baumann H, Levin SD, Puel A, Farr AG, Ziegler SF, Leonard WJ, and Lodish HF.** Cloning of a receptor subunit required for signaling by thymic stromal lymphopoietin. *Nat Immun* 1: 59–64, 2000.

21. **Park JH, Yu Q, Erman B, Appelbaum JS, Montoya-Durango D, Grimes HL, and Singer A.** Suppression of IL7Ralpha transcription by IL-7 and other prosurvival cytokines: a novel mechanism for maximizing IL-7-dependent T cell survival. *Immunity* 21: 289–302, 2004.
22. **Park LS, Martin U, Garka K, Gliniak B, Di Santo JP, Muller W, Largaespada DA, Copeland NG, Jenkins NA, Farr AG, Ziegler SF, Morrissey PJ, Paxton R, and Sims JE.** Cloning of the murine thymic stromal lymphopoietin (TSLP) receptor: formation of a functional heteromeric complex requires interleukin 7 receptor. *J Exp Med* 192: 659–670, 2000.
23. **Powrie F, Leach MW, Mauze S, Caddle LB, and Coffman RL.** Phenotypically distinct subsets of CD4+ T cells induce or protect from chronic intestinal inflammation in C. B-17 scid mice. *Int Immunol* 5: 1461–1471, 1993.
24. **Schluns KS, Kieper WC, Jameson SC, and Lefrancois L.** Interleukin-7 mediates the homeostasis of naive and memory CD8 T cells in vivo. *Nat Immun* 1: 426–432, 2000.
25. **Seddon B, Tomlinson P, and Zamoyska R.** Interleukin 7 and T cell receptor signals regulate homeostasis of CD4 memory cells. *Nat Immun* 4: 680–686, 2003.
26. **Suzuki K, Oida T, Hamada H, Hitotsumatsu O, Watanabe M, Hibi T, Yamamoto H, Kubota E, Kaminogawa S, and Ishikawa H.** Gut cryptopatches: direct evidence of extrathymic anatomical sites for intestinal T lymphopoiesis. *Immunity* 13: 691–702, 2000.
27. **Tan JT, Ernst B, Kieper WC, LeRoy E, Sprent J, and Surh CD.** Interleukin (IL)-15 and IL-7 jointly regulate homeostatic proliferation of memory phenotype CD8+ cells but are not required for memory phenotype CD4+ cells. *J Exp Med* 195: 1523–1532, 2002.
28. **Vivien L, Benoist C, and Mathis D.** T lymphocytes need IL-7 but not IL-4 or IL-6 to survive in vivo. *Int Immunol* 13: 763–768, 2001.
29. **Watanabe M, Ueno Y, Yajima T, Iwao Y, Tsuchiya M, Ishikawa H, Aiso S, Hibi T, and Ishii H.** Interleukin 7 is produced by human intestinal epithelial cells and regulates the proliferation of intestinal mucosal lymphocytes. *J Clin Invest* 95: 2945–2953, 1995.
30. **Watanabe M, Ueno Y, Yajima T, Okamoto S, Hayashi T, Yamazaki M, Iwao Y, Ishii H, Habu S, Uehira M, Nishimoto H, Ishikawa H, Hata J, and Hibi T.** Interleukin 7 transgenic mice develop chronic colitis with decreased interleukin 7 protein accumulation in the colonic mucosa. *J Exp Med* 187: 389–402, 1998.
31. **Watanabe M, Ueno Y, Yamazaki M, and Hibi T.** Mucosal IL-7-mediated immune responses in chronic colitis-IL-7 transgenic mouse model. *Immunol Res* 20: 251–259, 1999.
32. **Yamazaki M, Yajima T, Tanabe M, Fukui K, Okada E, Okamoto R, Oshima S, Nakamura T, Kanai T, Uehira M, Takeuchi T, Ishikawa H, Hibi T, and Watanabe M.** Mucosal T cells expressing high levels of IL-7 receptor are potential targets for treatment of chronic colitis. *J Immunol* 171: 1556–1563, 2003.

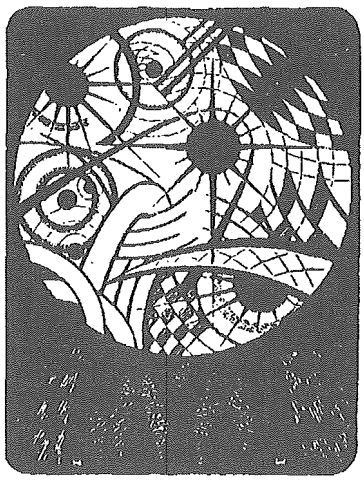

FEBS 29544 FEBS Letters 579 (2005) 2781–2787

IRF-1 mediates upregulation of LMP7 by IFN-γ and concerted expression of immunosubunits of the proteasome

Shin Namiki, Tetsuya Nakamura, Shigeru Oshima, Motomi Yamazaki, Yuko Sekine, Kiichiro Tsuchiya, Ryuichi Okamoto, Takanori Kanai, Mamoru Watanabe*

Department of Gastroenterology and Hepatology, Graduate School, Tokyo Medical and Dental University 1-5-45 Yushima, Bunkyo-ku, Tokyo 113-8519, Japan

Received 22 February 2005; revised 30 March 2005; accepted 1 April 2005

Available online 20 April 2005

Edited by Michael R. Bubb

Abstract **An immunoproteasome subunit low molecular weight protein 7 (LMP7) plays critical roles in major histocompatibility complex class I antigen processing; however, the mechanism for its expression has remained unclear. We demonstrate that interferon (IFN) regulatory factor-1 (IRF-1) has a pivotal role in IFN-γ-dependent LMP7 expression, as was shown for the other two immunosubunits. A tetracycline-inducible system for IRF-1 revealed its function in the LMP7 expression, and a genomic region functionally interacting with IRF-1 was also determined. Furthermore, the role of IRF-1 in IFN-γ-inducible LMP7 transcription was confirmed by employing small interfering RNA experiments and IRF-1−/− mice. These results suggest that IRF-1 acts as a master regulator for the concerted expression of immunoproteasome components.**

Keywords: Interferon regulatory factor-1; Low molecular weight protein 7; Low molecular weight protein 2; Multicatalytic endopeptidase complex-like 1; Immunoproteasome; Major histocompatibility complex class I antigen processing

1. Introduction

The proteasome plays an essential role in the processing of major histocompatibility complex class (MHC) I ligands [1] in most somatic cells to mediate immune responses against viruses and tumor cells [2]. Upon exposure of cells to interferon-γ (IFN-γ), three catalytic subunits of the proteasome, low molecular weight protein 7 (LMP7), LMP2, and multicatalytic endopeptidase complex-like 1 (MECL1), are expressed in company with each other [3–9]. These three "immunosubunits" replace the constitutive catalytic subunits, resulting in the formation of so-called immunoproteasomes, and alter the protein cleavage specificity so that more efficient class I antigen processing could be achieved [6–8,10–12].

There is increasing evidence that LMP7 plays pivotal roles in antigen presentation. Its effects on the peptidase specificity of the proteasome [11] or on efficient processing of several epitopes [13–15] were demonstrated by in vitro studies. Its role in antigen processing was also shown by in vivo experiments that employed LMP7-deficient mice [16]. In addition, studies have shown that the coexistence of LMP7 with the other immunosubunits facilitates the antigen presentation irrespective of its catalytic activity, indicating the importance of LMP7 for proper assembly of the immunoproteasome [15,17]. Therefore, investigating the regulatory mechanism for the expression of LMP7 and its mechanical association with those for the other two immunosubunits would have impacts on our understanding of the molecular basis for class I antigen processing; however, this issue has remained totally unclear. It was reported that IFN-γ-dependent expression of both LMP2 [18–20] and MECL1 [21] is regulated by a transcription factor IFN regulatory factor-1 (IRF-1), one among a variety of effector molecules in IFN-γ-mediated signaling that evokes a variety of immune responses [22,23]. Given a biological rationale for the finely tuned expression of the immunosubunits in response to IFN-γ and the presence of a common factor for this process, we were particularly interested in examining the role of IRF-1 in the induction of LMP7 by IFN-γ. We here show that IRF-1 serves as a transcriptional activator for LMP7 both in vitro and in vivo, indicating the central role of IRF-1 in the prerequisite step for the class I antigen processing.

2. Materials and methods

2.1. Cell culture

HeLa and human colonic epithelial DLD-1 cells were grown in DMEM supplemented with 10% fetal bovine serum and 1% penicillin–streptomycin. Two sublines of DLD-1, DLD-1/tetracycline (TET)-repressor (TR) cells and DLD-1/TR/IRF-1-tag cells, were established and grown as previously described [24]. Cells were seeded at a density of 3×10^5 cells/ml in the medium 36 h prior to each experiment and, when indicated, were stimulated with either 50 ng/ml of human IFN-γ (PeproTech, London, UK) or 100 ng/ml of doxycycline (DOX) (Clontech, Palo Alto, CA, USA).

*Corresponding author. Fax: +81 3 5803 0262.
E-mail address: mamoru.gast@tmd.ac.jp (M. Watanabe).

Abbreviations: IRF-1, interferon regulatory factor-1; IFN, interferon; LMP, low molecular weight protein; MECL1, multicatalytic endopeptidase complex-like 1; MHC, major histocompatibility complex; TET, tetracycline; DOX, doxycycline; RT-PCR, reverse transcriptase-polymerase chain reaction; G3PDH, glyceraldehyde-3-phosphate dehydrogenase; MIG, monokine induced by interferon-γ; siRNA, small interfering RNA; ChIP assay, chromatin immunoprecipitation assay; STAT, signal transducer and activator of transcription; TNF-α, tumor necrosis factor-α

0014-5793/$30.00
doi:10.1016/j.febslet.2005.04.012

2.2. Mice

Mice deficient in IRF-1 with a background of C57BL/6 [25], a kind gift of Dr. S. Taki (Shinshu University), and IRF-1+/+ mice derived from the heterozygous littermates were maintained under specific pathogen-free facility at Tokyo Medical and Dental University. All mice were genotyped and used at 20 weeks of age. For in vivo studies, mice were injected i.p. with 1×10^5 U per body of murine IFN-γ (PeproTech) or vehicle alone ($n = 2$ per group). After 6 h of injection, colon and liver samples from individual mice were isolated and subjected to total RNA extraction as described below. The institutional review board has approved our experimental animal studies.

2.3. Total RNA isolation and cDNA synthesis

Total RNA was isolated from the cultured cells or from the murine tissues by the standard protocol using Trizol reagent (Invitrogen, Carlsbad, CA, USA) according to the manufacturer's instructions. When required, RNA samples were subjected to cDNA synthesis as previously described [24], yielding a final volume of 21 μl from a total RNA aliquots of 5 μg.

2.4. Northern blot and RT-PCR

Northern blotting was carried out essentially as described previously [24] by using 13 μg of each total RNA sample. The cDNA probes for the human IRF-1, LMP7, LMP2, MECL1 and glyceraldehyde-3-phosphate dehydrogenase (G3PDH) genes were generated by RT-PCR. Primers were as follows: sense (S)-IRF-1, 5′-TTCCCTCTTCCACTCG GAGT-3′ and antisense (AS)-IRF-1, 5′-GATATCTGGCAGGGAGT TCA-3′ for IRF-1; S-LMP7-E2 (see below), 5′-ATGGCGCTACTA-GATGTATGCGGA-3′ and AS-LMP7-E1/E2 (see below), 5′-TTGAT TGGCTTCCCGGTACTGGTGC-3′ for LMP7; S-LMP2, 5′-GGA-GAGCGGTGCCTTGCAGGGATGC-3′ and AS-LMP2, 5′-CATTG CCCAAGATGACTCGATGGTC-3′ for LMP2; S-MECL1, 5′-CCA AGATGCTGAAGCCAGCCCTGGA-3′ and AS-MECL1, 5′-ATGT TCGGCTGGAACCGGTCTTCTA-3′ for MECL1; S-G3PDH, 5′-TGAAGGTCGGAGTCAACGGATTTGGT-3′ and AS-G3PDH, 5′-CATGTGGGCCATGAGGTCCACCAC-3′ for G3PDH. Hybridization was carried out at 42 °C overnight for the former four genes and at 68 °C for 2 h for G3PDH.

Two transcripts of the human LMP7 gene (LMP7-E1 and -E2) [26] were distinctively but simultaneously amplified by using multiplex semi-quantitative RT-PCR. To this end, another primer S-LMP7-E1 (5′-GGAAAGATTCAGAGACTGCGCCCT-3′) was designed in addition to aforementioned primers S-LMP7-E2 and AS-LMP7-E1/E2 so that each transcript could be specifically amplified with the pair of S-LMP7-E1/AS-LMP7-E1/E2 and of S-LMP7-E2/AS-LMP7-E1/E2, respectively (Fig. 1B, top). Each reaction mixture contained 1 μl of cDNA derived from either DLD-1 or DLD-1/TR/IRF-1-tag cells, 12.5 pmol of both S-LMP7-E1 and S-LMP7-E2 primers, and 25.0 pmol of AS-LMP7-E1/E2 primer in a 25-μl reaction containing 0.25 U of LA *Taq* polymerase (TaKaRa, Kyoto, Japan). The reaction consisted of denaturation at 94 °C for 30 s, annealing at 60 °C for 30 s, and extension at 72 °C for 30 s. Eighteen cycles of reaction was performed for both the multiplex PCR for LMP7 and conventional PCR for G3PDH, since the amplification for each gene was in the linear curve under these conditions. For control experiments, plasmids pGEM-LMP7-E1 and -E2 were created by inserting the PCR-amplified fragment with primer set of S-LMP7-E1 and AS-LMP7-E1/E2 or S-LMP7-E2 and AS-LMP7-E1/E2 into a pGEM-T Easy vector (Promega, Madison, WI, USA), respectively. Equal amount of these two plasmids were mixed and the PCR amplification was performed using 15 or 150 pg (7.5 or 75 pg for each plasmid) of the mixed DNA as a template.

For murine studies, the quantities of mRNA for IRF-1, LMP7, LMP2, MECL1, monokine induced by interferon-γ (MIG) and β-actin were determined by semi-quantitative RT-PCR. The primers and the cycle numbers for the amplification of each gene were as follows: S-IRF-1, 5′-ATGCCAATCACTCGAATGCG-3′ and AS-IRF-1, 5′-TGGTGCACAAGGAATGGCCT-3′ for IRF-1 (18 cycles); S-LMP7, 5′-CTCCGTGTCTGCAGCATCC-3′ and AS-LMP7, 5′-TCCA CTTTCACCCAACCGTC-3′ for LMP7 (23 cycles); S-LMP2, 5′-TC CACACCGGGACAACC-3′ and AS-LMP2, 5′-CCAGCCAGCTAC-TATGAGATGC-3′ for LMP2 (20 cycles); S-MECL1, 5′-CGTCT-GCCCTTTACTGC-3′ and AS-MECL1, 5′-CCACTTCATTCCACC-TCC-3′ for MECL1 (21 cycles); S-MIG, 5′-TGAAGTCCGCTGTTCT-TTTCCT-3′ and AS-MIG, 5′-TTATGTAGTCTTCCTTGAACGA-CG-3′ for MIG (27 cycles); S-β-actin, 5′-CCTAAGGCCAACCGT-GAAAAG-3′ and AS-β-actin, 5′-TCTTCATGGTGCTAGGAGC-CA-3′ for β-actin (20 cycles). PCR products were separated on 1.8% agarose gels, stained by ethidium bromide, and visualized by using a Lumi-Imager F1 system (Roche, Mannheim, Germany).

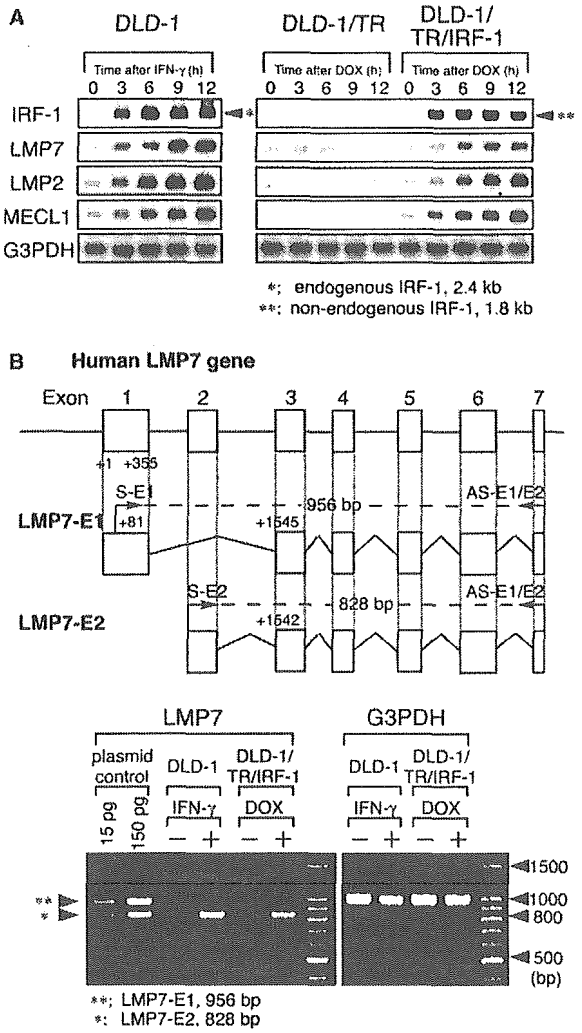

Fig. 1. Forced expression of IRF-1 upregulates expression of not only LMP2 and MECL1 mRNAs, but also LMP7 mRNA which encodes functional LMP7 protein. (A) Parental DLD-1 (DLD-1) or its sublines DLD-1/TR and DLD-1/TR/IRF-1-tag (DLD-1/TR/IRF-1) cells were stimulated with IFN-γ (50 ng/ml) or DOX (100 ng/ml), respectively, for indicated time periods. Total RNA was isolated and 13 μg of each was subjected to Northern blotting for IRF-1, LMP7, LMP2, MECL1 and G3PDH (loading controls) by using the ^{32}P-labeled cDNA probes. (B) Schematic diagram of the human LMP7 gene and its transcripts LMP7-E1 and -E2 (top) [26]. Nucleotide numbers were given with respect to the 5′ end of the LMP7-E1 (+1). The positions for the primers S-LMP7-E1 (S-E1), S-LMP7-E2 (S-E2) and AS-LMP7-E1/E2 (AS-E1/E2) are shown with arrows (top). DLD-1 or DLD-1/TR/IRF-1 cells were stimulated with IFN-γ (50 ng/ml) or DOX (100 ng/ml), respectively, collected before and after 12 h of stimulation for total RNA isolation, and then a semi-quantitative multiplex RT-PCR for LMP7 was carried out (bottom). As positive controls, equal amounts of the plasmids pGEM-LMP7-E1 and -E2 were mixed and the PCR was performed using 15 or 150 pg (7.5 or 75 pg for each plasmid) of the mixed plasmid as a template. The right panel shows the expression levels of the G3PDH gene as controls.

2.5. Western blot

Cells were harvested, washed twice in ice cold PBS and lysed in a buffer (50 mM Tris, pH 7.5, 5 mM $MgCl_2$, 1 mM EDTA, 0.5% Triton X-100, and complete protease inhibitor mix) for 15 min on ice. After centrifugation for 10 min, the supernatants were used as whole cell extracts. Eighty micrograms of DLD-1 extracts or 160 μg of HeLa extracts was analyzed by using anti-LMP7 (Affiniti, Mamhead, UK), anti-IRF-1 (Santa Cruz Biotechnology, Santa Cruz, CA, USA), and anti-β-actin (Sigma, Saint Louis, MO, USA) antibodies as described elsewhere [24]. Proteins were visualized with an ECL system according to the manufacturer's instructions.

2.6. ChIP assays

Chromatin immunoprecipitation (ChIP) assays were performed as described previously [24]. Briefly, after fixing DLD-1 cells with formaldehyde, soluble chromatin was extracted by sonicating the nuclei pellet obtained by cellular lysis. The sheared chromatin of ~500 bp was subjected to immunoprecipitation with anti-IRF-1 antibody or control IgG, and the co-immunoprecipitated DNA fragments were recovered by reversing cross-linking. Purified DNA was analyzed by quantitative PCR on a LightCycler system (Roche) by using six pairs of primers, each of which could amplify ~400 bp of the genomic DNA located in the vicinity of the 5′ part of the human LMP7 gene, to investigate the region extending ~2.5 kb in total (Fig. 3A, top). The following primers were used: S-1, 5′-GCTCCAGAATGAAAGCCTTCTCAG-3′, AS-1, 5′-GCCGGAAACATAAGAAACCACAGT-3′ for −957/−553 region; S-2, 5′-CGGCACACCAAACGGCCCACTGCC-3′, AS-2, 5′-TACTAGGCAATCCCGCCTACTGTT-3′ for −556/−148 region; S-3, 5′-AAATATCTCCCATTCAGGGAGGCC-3′, AS-3, 5′-CAACCAGAAGACTAGAAGTCAGCC-3′ for −148/+290 region; S-4, 5′-AAGCTGCGCCTTTAGATGACACGA-3′, AS-4, 5′-ATAGAGAAACTGTAGTGTCCTGGG-3′ for +291/+747 region; S-5, 5′-TATGCGATCTCCAGAGCTCGCTTT-3′, AS-5, 5′-TCATAGGTTTCCCAAGACACCACA-3′ for +745/+1118 region; S-6, 5′-ATGAAATTTGCCTGCTGGCCTCCT-3′, AS-6, 5′-GGAAGAATTCTGTGGGCTGATAAG-3′ for +1115/+1560 region. The nucleotide number was assigned relative to the transcription start site of the LMP7-E1 transcript [26]. By using software provided by the manufacturer, the amount of DNA fragment in each sample was calculated relative to the standard curve obtained by the three different dilutions of input DNAs (10%, 1% and 0.1%). Three independent chromatin preparations were made, and the average value obtained for each sample was indicated as a percentage of total input DNA.

2.7. Reporter plasmid construction, transient transfection and reporter assays

The LMP7-wild-type (wt)-Luc construct was made by inserting the PCR-amplified genomic DNA fragment corresponding to the nucleotide from −100 to +1601 of the human LMP7 gene into a pGL3-Basic plasmid (Promega). The LMP7-mutant (mt)-Luc containing a 4-bp mutation within the IRF-E at +581/+592 was constructed by PCR-mediated mutagenesis. Wild-type sequences and the introduced mutations within the IRF-E were given with top strand sequences as follows: wt, +581GCTTTCGCTTTC+592; mt, +581GCCCTCGCCCTC+592 (underlined residues indicate introduced mutations). Either 5 μg of a pGL3-basic, LMP7-wt-Luc or LMP7-mt-Luc plasmid along with 0.03 μg of a *Renilla* luciferase reporter plasmid pRL-TK-Luc (Promega), and either 0.1 μg of an expression vector pcDNA3-IRF-1 [24] or a pcDNA3 (Invitrogen) were transiently transfected into HeLa cells by using TransIT-LT1 transfection reagent (Mirus, Madison, WI, USA). After transfection, cells were cultured in the presence or absence of IFN-γ (50 ng/ml) for 24 h. The determination of luciferase activities and the data normalization were performed as described previously [24].

2.8. siRNA experiments

DLD-1 and HeLa cells were transfected with either small interfering RNA (siRNA) oligonucleotides specific for human IRF-1 or control oligonucleotides with nonsense sequence for 12 h as described previously [24]. After the removal of the siRNA-containing medium, cells were cultured for an additional 12 h under the usual conditions, and then the medium was exchanged with either medium alone or that containing 50 ng/ml of human IFN-γ. Cells were collected after 24 h of the medium exchange, and the whole cell extracts were isolated and subjected to Western blot analysis for IRF-1, LMP7, and β-actin.

3. Results

3.1. Both IFN-γ and IRF-1 upregulate mRNA expression of the immunosubunits including LMP7

To examine the mechanism of inducible expression of LMP7 by IFN-γ, we initially analyzed human colonic epithelium-derived DLD-1 cells in which IFN-γ could elicit several cellular responses such as production of cytokines [24,27]. When expressions of LMP7, LMP2 and MECL1 were tested by Northern blotting, mRNA of all these components of the immunoproteasome was induced by IFN-γ (Fig. 1A, left). Since the kinetics of mRNA expression in response to IFN-γ was similar among these genes, it appeared likely that the transcription of each gene is analogously regulated by IFN-γ-dependent signaling events. Previous studies demonstrated that both LMP2 and MECL1 are transcriptionally regulated by IRF-1 [18–21]. We, therefore, hypothesized that IRF-1-mediated transcription might be also involved in IFN-γ-dependent LMP7 expression. To test this, we utilized a subline DLD-1/TR/IRF-1 cells where the expression of IRF-1 was conditionally regulated by use of the TET-on system [24]. As shown in Fig. 1A (right), expression of IRF-1 mRNA was efficiently induced and reached a maximum level within 3 h of the DOX addition in these cells, whereas no induction was observed in control DLD-1/TR cells. Of note, this transcript of IRF-1, originating from an artificially integrated gene, was different in size (~1.6 kb; shown with **) from that derived from the endogenous one that could be induced by IFN-γ (~2.4 kb; shown with *) (Fig. 1A, left). Hybridization with a probe for either LMP2 or MECL1 showed a marked induction of these mRNAs, confirming the pivotal role of IRF-1 in the transcription of both genes [18–21]. Intriguingly, following the expression of IRF-1, a significant increase of the LMP7 mRNA was also observed. In addition, this increase, seen from 3 to 12 h after stimulation with DOX, quite paralleled that of LMP2 and MECL1 mRNAs. These results suggested that the upregulation of LMP7 by IFN-γ might be mediated by a direct mechanism involving the IRF-1-mediated transcription.

3.2. Both IFN-γ and IRF-1 predominantly induce expression of LMP7-E2 between two species of the human LMP7 mRNA

The human LMP7 gene codes for two alternative forms of mRNAs, LMP7-E1 and LMP7-E2, that differ in their 5′ regions encoding amino-terminal prosequences (Fig. 1B, top) [26]. It was, however, demonstrated that only LMP7-E2 gives rise to a functional protein that can be assembled into the proteasome, possibly reflecting the crucial role of the amino-terminal region in the following protein processing [28]. The probe used in our Northern blotting, derived from the LMP7-E2 cDNA, broadly encompassed the common sequence for both transcripts and, therefore, the observed bands should represent the expression levels of both mRNA species. However, it was also reported that the sizes of the two transcripts were indistinguishable in Northern blot analysis [26]. Thus, we next examined the content of these two mRNAs by using multiplex RT-PCR allowing one-tube amplification of cDNAs derived from both transcripts. As shown in Fig. 1B (bottom), amplification with a sense primer specific for LMP7-E2 (S-E2) along with an antisense primer common for both LMP7-E1 and -E2 (AS-E1/E2) yielded the product of the expected size (828 bp) from the mRNA of unstimulated DLD-1 cells. By contrast,